

Challenging the Presence of Scalar Charge and Dipolar Radiation in Binary Pulsars

Kent Yagi,^{1,2} Leo C. Stein,^{3,4} and Nicolás Yunes²

¹*Department of Physics, Princeton University, Princeton, NJ 08544, USA.*

²*Department of Physics, Montana State University, Bozeman, MT 59717, USA.*

³*TAPIR, Walter Burke Institute for Theoretical Physics, MC 350-17,*

California Institute of Technology, Pasadena, CA 91125, USA

⁴*Cornell Center for Astrophysics and Planetary Science (CCAPS), Cornell University, Ithaca, NY 14853, USA*

(Dated: February 8, 2022)

Corrections to general relativity that introduce long-ranged scalar fields which are non-minimally coupled to curvature typically predict that neutron stars possess a non-trivial scalar field profile anchored to the star. An observer far from a star is most sensitive to the spherically-symmetric piece of this profile that decays linearly with the inverse of the distance to the source, the so-called *scalar monopole charge*, which is related to the emission of dipolar radiation from compact binary systems. The presence of dipolar radiation has the potential to rule out or very strongly constrain extended theories of gravity. These facts may lead people to believe that gravitational theories that introduce long-ranged scalar fields have already been constrained strongly from binary pulsar observations. Here we challenge this “lore” by investigating the decoupling limit of Gauss-Bonnet gravity as an example, in which the scalar field couples linearly to the Gauss-Bonnet density in the action. We prove a theorem that neutron stars in this theory can not possess a scalar charge, due to the topological nature of the Gauss-Bonnet density. Thus Gauss-Bonnet gravity evades the strong binary pulsar constraints on dipole radiation. We discuss the astrophysical systems which will yield the best constraints on Gauss-Bonnet gravity and related quadratic gravity theories. To achieve this we compute the scalar charge in quadratic gravity theories by performing explicit analytic and numerical matching calculations for slowly-rotating neutron stars. In generic quadratic gravity theories, either neutron star-binary or neutron star-black hole systems can be used to constrain the theory, but because of the vanishing charge, Gauss-Bonnet gravity evades the neutron star-binary constraints. However, in contrast to neutron stars, black holes in Gauss-Bonnet gravity do anchor scalar charge, because of the difference in topology. The best constraints on Gauss-Bonnet gravity will thus come from accurate black hole observations, for example through gravitational waves from inspiraling binaries or the timing of pulsar-black hole binaries with radio telescopes. We estimate these constraints to be a factor of ten better than the current estimated bound, and also include estimated constraints on generic quadratic gravity theories from pulsar timing.

PACS numbers: 04.50.Kd 04.20.Gz 04.70.Bw 97.60.Gb

I. INTRODUCTION

Almost a century since Einstein’s discovery of his general theory of relativity (GR), we continue to test it and wonder whether it is right in unexplored regimes. Perhaps the most famous of these tests are those carried out in the solar system [1], which not only confirmed the theory initially, but also served to rule out a plethora of modified models in the 1970s. The solar system, however, is an unsuitable place to test the strong, dynamical, and non-linear features of the gravitational interaction [2]. Gravity is simply too weak and the velocities of planets are simply too small relative to the speed of light within the solar system.

On top of that, astrophysical observations and theoretical studies have sparked a renewed interest in corrections to GR. The observations of galactic rotation curves have been used to pose certain modifications to Newtonian dynamics [3–6]. Corrections to GR on cosmological length scales have been invoked to attempt to explain the observation of late-time acceleration of the universe [7–9]. Quantum gravitational theories, like string theory, will induce corrections to GR in their low-energy effective

theories [10–12]. The low-energy effective theories of loop quantum gravity and inflation, for example, predict corrections to GR in the form of curvature-squared and higher operators [13–18].

Enter binary pulsars. With some of the strongest gravitational fields in the universe, neutron stars (NSs) are spectacular laboratories to test strong gravity. Neutron stars can rotate at fantastic speeds, sometimes with millisecond spin periods, and their emission can be detected as pulses in the radio band. When in a binary system, the pulses’ arrival times are modulated, encoding rich information about the properties of the orbit, and thus, of the nature of gravity. Since the discovery of the Hulse-Taylor binary pulsar, many others have been used to stringently constrain any deviations from the predictions of Einstein [19–23]. Some of these consist of two NSs, like the Hulse-Taylor binary, while others consist of a white dwarf (WD) and a NS. Typical orbital periods are on the order of several hours to days.

Over the past 50 years, binary pulsars have been used to invalidate many a modified gravity theory, and some people in the community may think that modified gravity theories with long-ranged scalar fields can be very well-constrained with binary pulsar observations because

they lead to the emission of dipolar radiation in binary systems. Such radiation is absent in GR because of the conservation of certain Noether charges (a curved-space version of mass and linear momentum). Long-ranged scalar fields in modified gravity do not typically have such conservation laws, and thus, they may carry energy and momentum away from the binary system in a monopolar or dipolar fashion if excited. If so, the orbital period decay would be much faster than that predicted in GR. An observation consistent with GR would thus lead to a stringent constraint on such a theory.

In this paper, we show explicitly and in great detail that this lore is not always correct. The presence or absence of dipole radiation in modified gravity when modeling binary systems depends sensitively on the structure of the scalar field that is excited by the compact objects that form the binary. Far away from the compact objects, the scalar field can be decomposed in spherical harmonics, and the spherically symmetric ($\ell = 0$), $1/r$ fall-off shall be called the *scalar monopole charge* or *scalar charge* for short. When a member of a binary system possesses such a scalar charge, dipole radiation is typically excited; when scalar charge is absent in both binary constituents, dipole radiation is heavily suppressed [24, 25].¹ For example, such a suppression is present in a particular quadratic gravity theory, dynamical Chern-Simons (dCS) gravity [14, 26]. In dCS, the scalar charge of an isolated body is suppressed by parity considerations, and therefore dipolar radiation from a binary is also heavily suppressed [27, 28]. A similar absence of the stellar scalar charge and the suppression of dipolar radiation of stellar binaries are found in shift-symmetric Horndeski theories [29], a certain class of generic scalar-tensor theories with up to second derivatives in the field equations. Shift-symmetric theories are those whose field equations remain unchanged upon a constant shift of the scalar field

We formalize the above through a *miracle hair loss* conjecture and theorem. This conjecture is aimed at establishing that gravity theories with a shift-symmetric, long-ranged scalar sourced by a linear (non-derivative) coupling to a topological density do not activate a scalar charge in NSs. A topological density is one which when integrated over the manifold yields a topological invariant. We rigorously prove such a theorem for a particular modified gravity theory that has the above properties: dynamical Gauss-Bonnet (DGB) gravity in the so-called decoupling limit [30] (here abbreviated D²GB). This theory modifies the action by adding a term that is the product of a dynamical scalar field with the Gauss-

Bonnet topological density. The integral of the latter is a topological invariant, i.e. the Euler characteristic of the manifold, and the theory is manifestly shift-symmetric. Such a theorem has long-ranging implications, since the absence of a scalar charge in isolated neutron stars automatically implies that dipolar radiation is highly suppressed in binary systems. This renders pulsar binaries ineffective at constraining such theories.

We should point out that this theorem only applies to ordinary stars, such as NSs, and not to black holes (BHs). For example, the scalar charge of a BH in D²GB gravity has been explicitly calculated and found to be non-vanishing in [24, 30–33]. This situation is in direct contrast to the no-hair theorems of scalar-tensor theories [34–36] of the Jordan-Brans-Dicke variety (or, more generally, the Bergmann-Wagoner type [37, 38]; we will continue to refer to this class of theories as simply “scalar-tensor” theories). These theorems prove that in scalar-tensor theories, stationary, isolated BHs in vacuum have no scalar hair, and thus, in particular no scalar charge. Possible ways to grow BH scalar hair are to introduce a potential for the scalar field [39] or to impose certain cosmological boundary conditions [40, 41]. The latter has been dubbed Jacobson’s *miracle hair growth* formula for BHs in scalar-tensor theories [40, 41]. On the other hand, NSs in scalar-tensor theories do generically possess a scalar charge, as this is sourced by the matter stress-energy tensor [42–46]. It is this fact that makes scalar-tensor theories easy to constrain with binary pulsar observations. A similar absence of black hole scalar charges has recently been shown in shift symmetric Horndeski theories except for D²GB gravity in [47, 48].

We demonstrate this theorem at work by computing the scalar charge explicitly in D²GB, as well as in theories that violate the conditions of the theorem, wherein the scalar charge is non-vanishing. We first compute the scalar charge analytically for slowly-rotating NSs in a post-Minkowskian expansion, i.e. an expansion in the ratio of the stellar mass to its radius (the stellar compactness) and with simple equations of state. We then compute the scalar charge numerically without a post-Minkowskian expansion and with more realistic equations of state. We verify that in the limit where quadratic gravity approaches D²GB, the scalar charge vanishes linearly with the coupling constants. Theories which don’t satisfy the conditions of the theorem need not have a particularly large or small scalar charge. In fact in our explicit calculations, we show examples of strong dependence on coupling parameters and the compactness of a body. This may lead to suppression of scalar charge in some theories, though it is still present.

The miracle hair loss theorem/conjecture is so powerful that it allows us to easily predict which binary systems will be best to test which theory. Generically, if scalar charge is activated, then the observation of WD/NS or NS/NS pulsar binaries with radio telescopes is already sufficient to strongly constrain the particular modified theory. On the other hand, if the conjecture is applicable,

¹ The dipole radiation is suppressed in the post-Newtonian (PN) sense: it may be present, but will appear at a higher order in powers of v/c than one would naively expect, which would be -1 PN relative to the GR quadrupolar radiation. This is distinct from the suppression of dipole radiation in a NS/NS system in Brans-Dicke type theories, which comes about because the dipolar radiation depends on the difference in sensitivities of the two bodies.

Theory	Scalar charge		Estimated upper bound on $\sqrt{ \alpha }$ [km]				Current estm. bound [km]
	NS	BH	NS/WD	NS/NS	NS/BH	BH/BH	
D ² GB	✗	✓	✗	✗	(0.12)	(3.4)	1.9 [49]
TEdGB	✓	✓	1–2	1.5–3.5	(0.12)	(3.4)	1.4 [50, 51]
Kretsch.	✓	✓	0.06–0.1	0.15–0.45	(0.03–0.07)	(3.4)	1.9 [49]

TABLE I. Summary of whether certain modified theories activate a scalar charge in NSs and BHs, and the estimated bounds on the coupling parameter $\sqrt{|\alpha|}$ from a variety of systems. We consider truncated Einstein-dilaton-Gauss-Bonnet gravity (TEdGB) and the decoupling limit of any Gauss-Bonnet theory (D²GB), as well as a certain quadratic gravity theory in which the scalar field does not couple to a topological density (Kretschmann). Quantities in parentheses represent projected bounds using systems that have not yet been observed, but which may be observed in the near future with radio/GW observations. Note that a NS/BH system could produce the best constraint within each theory.

and scalar charge is not activated in NSs but is activated in BHs, one requires BH binaries or mixed BH/NS binaries to place a constraint. The former could be detected through their gravitational waves (GWs) by ground-based interferometers, such as LIGO and Virgo [52–57], while the latter may be detected in future radio telescopes, such as the Square Kilometer Array [58]. The conjecture, for example, can easily be applied to quadratic gravity theories which *naturally* avoid solar system constraints (since quadratic curvature densities are small in the solar system) [59–64], yet predict strong modifications to GR when the curvature is large, such as around NSs and BHs [24, 27, 65–73]. Table I shows a few examples of such theories, whether they activate a scalar charge in NSs and BHs, which systems are best to constrain them and an estimate of how well they can be constrained.

The remainder of this paper deals with the details of the results explained above. Section II reviews the basics of quadratic gravity. Section III states and proves the miracle hair loss theorem. Section IV presents an analytical and a numerical demonstration of the theorem. Section V estimates binary pulsar and GW constraints due to dipolar radiation. Section VI concludes and points to future research. All throughout, we use geometric units in which $G = 1 = c$.

II. THE ABC OF QUADRATIC GRAVITY

Here we review and classify quadratic gravity theories, mainly following the presentation of [14, 25, 30]. We begin with a description of the motivation for studying such theories. This will set up the stage for the introduction of our classification. We then conclude with a discussion of well-posedness in these theories and current constraints. As we classify theories, we will come across a few theories that we will investigate in detail in this paper; the actions that define these theories will have their equations marked with (\star).

A. Motivation

Our focus is theories that correct GR through higher-curvature terms in the action and include long-ranged scalar fields. The scalar field of interest must be of “gravitational strength,” i.e. should couple to matter weakly, although it is allowed to couple directly to curvature. As such, these theories will be *metric*, with matter coupling directly only to the metric tensor, and the scalar field coupling to the metric through curvature, and thus indirectly to matter.

These theories are motivated from at least two places. First, from the modern bottom-up, effective field theory (EFT) standpoint, we should expect GR to acquire corrections at some length scale. At low energies, these potential corrections can be described at the level of the action via an expansion in powers of the Riemann curvature tensor. If truncating at first order in curvature, we recover GR, with the Einstein-Hilbert action

$$S_{\text{EH}} = \kappa \int d^4x \sqrt{-g} R, \quad (1)$$

where g is the determinant of g_{ab} , $R = g^{ab}R_{ab} = g^{ab}R_{acb}{}^c$ is the Ricci scalar, and $\kappa = (16\pi G)^{-1}$.

If we include scalar fields, then at this order we for example arrive at Jordan-Brans-Dicke theory [74, 75], where the scalar field is linearly coupled to the Ricci scalar in the Jordan frame. Jordan-Brans-Dicke theory allows for gross modifications from GR in the form of long-ranged scalar charges and scalar dipole radiation, which are strongly constrained from solar system and binary pulsar observations [1, 76]. Furthermore, it is always possible, through a conformal transformation [77], to go to the Einstein frame of the theory, where the linear-in-curvature term in the action is simply the Einstein-Hilbert term of Eq. (1). At next order in curvature, we arrive at quadratic gravity theories, which are the topic of this paper.

The second motivation for such theories is from the top-down, high-energy theory viewpoint. Fundamental theories of quantum gravity (such as string theory and loop quantum gravity) will induce both higher-corrections to GR and a number of scalar fields, which

may be long-ranged [16, 32, 78–82]. For example, in heterotic string theory and in the string frame in D dimensions, the next-to-leading order correction to GR in a low-curvature expansion (first derived in [79]) is given (in the notation of [83]) by

$$S = \frac{1}{2\kappa_D^2} \int d^D \hat{x} \sqrt{|\hat{g}|} e^{-2\hat{\phi}} \left[\hat{R} + 4(\hat{\partial}\hat{\phi})^2 + \frac{\alpha'}{8} \left(\hat{R}^2 - 4\hat{R}_{ab}\hat{R}^{ab} + \hat{R}_{abcd}\hat{R}^{abcd} + \dots \right) \right], \quad (2)$$

where \dots stand for higher-order in curvature terms. Here, ϕ is the dilaton, α' is the Regge slope parameter, κ_D^2 is the D -dimensional gravitational strength, and $\hat{\cdot}$ represents a quantity in the string frame. The theory described by the action in Eq. (2) is referred to as *Einstein-dilaton-Gauss-Bonnet* (EdGB). Through a conformal transformation and a field redefinition, this can be cast in the Einstein frame (in the notation of [83]) as

$$S = \frac{1}{2\kappa_D^2} \int d^D x \sqrt{|g|} \left[R - \frac{1}{2}(\partial\phi)^2 + \frac{\alpha'}{8} e^{-\gamma\phi} \left(R^2 - 4R_{ab}R^{ab} + R_{abcd}R^{abcd} + \dots \right) \right], \quad (3)$$

where $\gamma = \sqrt{2/(D-2)}$ and again the \dots stand for higher order terms, but in both curvature and the scalar field. If such higher order terms are dropped from the action, the resulting theory is called *truncated Einstein-dilaton-Gauss-Bonnet* (TEdGB) [83].

In string theory, one can work in dimensions higher than 4, but henceforth in this paper, we will focus only on theories that have already been compactified to 4 dimensions. This compactification introduces a large number of dynamical degrees of freedom (moduli fields), such as the dilaton and axion(s). The resulting low-energy effective action may be truncated to a specific operator order, and this truncation may affect the field content of the effective action. Performing this truncation consistently is not trivial [84]. Here we focus only on the metric and long-ranged scalar sector of such a theory.

B. Classification

Let us define *quadratic gravity* theories through the action

$$S = S_{\text{EH}} + S_{\text{mat}} + S_\vartheta + S_q, \quad (4)$$

where the Einstein-Hilbert term S_{EH} was given in Eq. (1), S_{mat} is the action of any matter fields that do not depend on the scalar field, and S_ϑ is the action for a canonical scalar field with potential U ,

$$S_\vartheta = -\frac{1}{2} \int d^4 x \sqrt{-g} [(\nabla_a \vartheta)(\nabla^a \vartheta) + 2U(\vartheta)]. \quad (5)$$

This form for the action is always possible in an appropriate conformal frame and through field redefinitions [77].

The quadratic part of quadratic gravity comes from

$$S_q = \int d^4 x \sqrt{-g} F[R_{abcd}, \vartheta, \partial R_{abcd}, \partial \vartheta, \dots], \quad (6)$$

where $F[\cdot]$ is the *interaction density* between the scalar field and the curvature, which must be homogeneous of degree 2 in the curvature tensor (and its derivatives). This means that for any real constant λ ,

$$F[\lambda R_{abcd}, \dots] = \lambda^2 F[R_{abcd}, \dots]. \quad (7)$$

This property does not allow the interaction density to depend on terms independent of or linear in the Riemann tensor.

The field equations of quadratic gravity can be obtained by varying the full action with respect to the metric tensor and the scalar field. The latter leads to the scalar evolution equation

$$\square \vartheta - U'(\vartheta) = -\frac{\partial F}{\partial \vartheta} + \nabla_a \frac{\partial F}{\partial (\nabla_a \vartheta)} - \dots, \quad (8)$$

where the right-hand side is minus the variational derivative of S_q with respect to ϑ . This is a particularly simple wave equation when $U = 0$ and when F is linear in the scalar field (and its derivatives).

The space of quadratic gravity theories is spanned by the functional degree of freedom in the interaction density, which makes this space extremely large. There are several non-exclusive ways to classify the types of interaction densities that may appear within S_q in ways that are relevant to the phenomenology of the theories. We now provide a partial classification on the basis of three properties:

- having derivative or non-derivative interactions,
- coupling to a topological density or not, and
- possessing a shift symmetry or not.

This classification is summarized in Fig. 1, a figure we will return to in the following subsections when we define and discuss each of the above items in detail.

1. Derivative and Non-derivative Interactions

For the purposes of this paper, a *derivative interaction* is one that depends on at least one derivative of the scalar field or of the Riemann tensor. From the EFT viewpoint, derivative interactions are higher operator order and should be suppressed relative to non-derivative (algebraic) interactions—unless for some reason only derivative interactions appear (for example, to enforce a shift symmetry).

Given this, let us focus on non-derivative interactions. The interaction density must then be a sum of terms of the form

$$F[R_{abcd}, \vartheta] = \sum_i f_i(\vartheta) A_i[R_{abcd}], \quad (9)$$

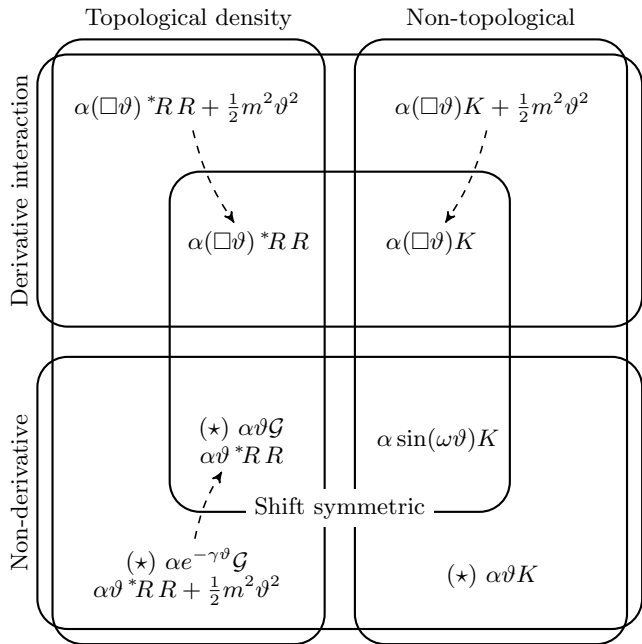


FIG. 1. A classification of corrections to GR which are at most quadratic in curvature and couple to a single dynamical scalar field ϑ . The interaction density may explicitly include derivatives (top half), or may be a non-derivative interaction (bottom half). The combination of curvature tensors to which the scalar is coupled may be of a topological nature (like the Pontryagin or Gauss-Bonnet scalars; left half), or may be unrelated to topological invariants (right half). In all of these sectors, an interaction may enjoy a continuous or discrete shift symmetry (inner region), or it may not (outer region). Some of these interactions are limiting cases of others, e.g. when an explicit mass vanishes $m \rightarrow 0$, a shift symmetry can be acquired. The theories we investigate in detail in this paper are marked with (\star) .

where $f_i(\vartheta)$ are ordinary functions of ϑ , and every component of $A_i[R_{abcd}]$ is a scalar function that is homogeneous of degree 2, and now depends only on the Riemann tensor but not its derivatives. In the units we are using, the $f_i(\vartheta)$ have dimensions of length squared. If so desired, they can be made dimensionless by pulling out some coefficients α_i with dimensions of length squared, i.e.

$$f_i(\vartheta) = \alpha_i \bar{f}_i(\vartheta), \quad (10)$$

with \bar{f}_i dimensionless.

At first degree in curvature, there is only one scalar curvature invariant, the Ricci scalar R . At quadratic degree there are only four independent scalar curvature invariants,

$$R^2, \quad R_{ab}R^{ab}, \quad K, \quad {}^*R R, \quad (11)$$

where the Kretschmann scalar is $K \equiv R_{abcd}R^{abcd}$, the Pontryagin density is ${}^*R R \equiv {}^*R_{abcd}R^{abcd}$, with the (left) dual of the Riemann tensor defined as

$${}^*R^{ab}{}_{cd} = \frac{1}{2} \epsilon^{abef} R_{efcd}, \quad (12)$$

and where ϵ_{abcd} is the Levi-Civita tensor. All other quadratic curvature invariants are algebraically dependent on the four in (11). For example, using the Weyl tensor C_{abcd} , we have that ${}^*C_{abcd}C^{abcd} = {}^*R R$; similarly, an appropriate contraction of two copies of the left-dual Riemann tensor ${}^*R R$ is proportional to both the Euler density and what is typically referred to as the four-dimensional Gauss-Bonnet density \mathcal{G} ,

$${}^*R R \equiv {}^*R_{abcd} {}^*R^{cdab} = -\mathcal{G}, \quad (13)$$

$$\mathcal{G} \equiv R^2 - 4R_{ab}R^{ab} + R_{abcd}R^{abcd}. \quad (14)$$

Given all of this, when we restrict ourselves to quadratic gravity theories with non-derivative interactions, the most general form of S_q is given by

$$S_q = \int d^4x \sqrt{-g} [f_1(\vartheta)R^2 + f_2(\vartheta)R_{ab}R^{ab} + f_3(\vartheta)R_{abcd}R^{abcd} + f_4(\vartheta)R_{abcd}{}^*R^{abcd}]. \quad (15)$$

Some examples of these are presented in the bottom rectangular box of Fig. 1.

If the coupling between the scalar and curvature is large, the terms in Eq. (15) can drastically affect the theory. For example, at strong coupling, the Pontryagin coupling can make the graviton kinetic term flip sign at high k -number, becoming a ghost field [85]. However, in the EFT context, this only occurs outside the regime of validity of the theory [86]. We discuss this further in Sec. II C.

When considering derivative interactions without any further restrictions, a plethora of terms could be written for the interaction density. Some examples are presented in the top rectangular box of Fig. 1. Note, of course, that many other terms could also be written down. For example, derivative interactions could also include terms proportional to products of derivatives of the scalar field with the Ricci tensor or scalar. We mention derivative interactions for pedagogical reasons and for completeness of the classification, but we will not study them in this paper in detail.

2. Topological/non-topological density

Let us define a *topological interaction* as one that is the product of a function of the scalar field and a *topological density* T_i :

$$F[R_{abcd}, \vartheta, \dots] = \sum_i \bar{F}_i[\vartheta, \partial\vartheta, \dots] T_i, \quad (16)$$

where each functional \bar{F}_i is now independent of the curvature tensor. A topological density is defined as a quantity whose volume integral over the four-dimensional manifold is a topological invariant. For example, the Euler density, which is proportional to \mathcal{G} (see Sec. III for the exact relationship), is a topological density because its volume integral is proportional to the Euler

characteristic χ . Similarly, the Pontryagin density $*RR$ is also a topological density because its volume integral is proportional to the first Pontryagin number.

An important property of topological densities is that in a simply-connected neighborhood, each may be written as the divergence of a 4-current. For example, in the Pontryagin case,

$$*RR = \nabla_a J^a, \quad (\text{locally}) \quad (17)$$

and similarly for \mathcal{G} . This allows for the local integration by parts of such interactions, which explains why, in the absence of a scalar field, they do not lead to modifications to the classical field equations.

Thus, when we restrict ourselves to quadratic gravity theories with non-derivative, topological interactions, the most general form of S_q is

$$S_q = \sum_i \int d^4x \sqrt{-g} f_i(\vartheta) T_i, \quad (18)$$

which we define as *topological quadratic gravity* (though this is unrelated to topological quantum field theory or to topological massive gravity [87, 88]). A few examples of topological quadratic gravity theories are presented in the intersection of the left and bottom rectangles of Fig. 1. For simplicity, let us consider the case in which the scalar field couples only to a single topological density. Then, when $T = *RR$, S_q defines *dynamical Chern-Simons* (DCS) gravity, and when $T = \mathcal{G}$ it defines *dynamical Gauss-Bonnet* (DGB) gravity. The specific choice

$$(\star) \quad S_{\text{TEdGB}} = \int d^4x \sqrt{-g} \alpha_{\text{TEdGB}} e^{-\gamma\vartheta} \mathcal{G} \quad (19)$$

recovers *truncated Einstein-dilaton-Gauss-Bonnet* (TEdGB) theory in 4 dimensions [83], where ϑ plays the role of the dilaton and $(\alpha_{\text{TEdGB}}, \gamma)$ are constant coupling strengths. Later in this paper, we will study TEdGB in more detail, which is why we have marked it with (\star) . The full action for TEdGB is given by the sum of the Einstein-Hilbert term (1), the kinetic term action for ϑ with vanishing potential (5), and the interaction term above, viz. $S = S_{\text{EH}} + S_{\vartheta} + S_{\text{TEdGB}}$.

An important property of these theories is that any constant shift or offset, $f(\vartheta) \rightarrow f(\vartheta) + c$, in Eq. (18) does not affect the classical equations of motion (EOMs), since it only contributes a constant multiple of a topological number to the action. Equivalently, since T can locally be written as a divergence, upon variation of the action, this shift only contributes a boundary term. Thus, without loss of generality, we may shift $f(\vartheta)$ such that $f(0) = 0$, so that if $f(\vartheta)$ is expanded as a Taylor series, the expansion starts at first order in ϑ .

Expanding $f(\vartheta)$ in a Taylor series is appropriate in the so-called *decoupling limit* of a theory, where the modifications to GR are sufficiently small. This can be enforced, for example, by requiring that $f(\vartheta)$ satisfy

$$f(\vartheta) T \ll \kappa R, \quad (20)$$

where we recall that, for example, $T = *RR$ or $T = \mathcal{G}$. In this case, we say that the scalar ϑ “decouples and interacts weakly.” In fact, if the theory is treated as an EFT, we expect the action to contain terms at higher order in α . In this case, the solution ϑ should also be expanded in a power series in α ; sub-leading terms in this expansion could be corrected by higher- α terms in the action, so they may not be trusted. Thus, to be consistent, if one ignores $\mathcal{O}(\alpha^2)$ terms in the action, one must also ignore $\mathcal{O}(\alpha^2)$ terms in the solution for ϑ .

So long as $f'(0) \neq 0$, all choices of coupling functions yield the same two theories, *decoupled dynamical Gauss-Bonnet* (D²GB) and *decoupled dynamical Chern-Simons* (D²CS), with actions²

$$(\star) \quad S_{\text{D}^2\text{GB}} = \int d^4x \sqrt{-g} \alpha_{\text{GB}} \vartheta \mathcal{G}, \quad (21)$$

$$S_{\text{D}^2\text{CS}} = -\frac{1}{4} \int d^4x \sqrt{-g} \alpha_{\text{CS}} \vartheta *RR, \quad (22)$$

where each α_X is constant (and the factor of $-1/4$ in $S_{\text{D}^2\text{CS}}$ is conventional). D²GB is another theory that we will study in more detail later in this paper, which is why we have marked it with (\star) .

When considering quadratic gravity theories with non-topological interactions, many other terms may be written down. Some examples are provided in the right rectangle of Fig. 1. Those examples consist of an interaction that is the product of a function of the scalar field and the Kretschmann scalar K , which is not a topological invariant. For future convenience, let us define the theory with S_q given by

$$(\star) \quad S_{\text{K}} = \int d^4x \sqrt{-g} \alpha_{\text{K}} \vartheta K \quad (23)$$

as *Kretschmann gravity*, where again α_{K} is a constant. This is another theory we will investigate in some detail later on, which is why we have marked it with (\star) . Of course, the function of the scalar field could depend on its derivatives. This paper will not focus on such theories any further, but we include them in Fig. 1 for completeness of the classification.

3. Shift symmetry

Let us define *shift-symmetric* theories as those whose equations of motion are invariant under the (discrete or continuous) shift $\vartheta \rightarrow \vartheta + c$, for a constant c . Quadratic gravity theories with non-derivative, topological interactions that depend on a linear coupling

² These theories have sometimes been referred to as “Einstein-dilaton-Gauss-Bonnet” gravity and “dynamical Chern-Simons” gravity elsewhere in the literature [14, 30, 89]; we have here changed the terminology to distinguish between other similar theories.

function, i.e. $f(\vartheta) = \alpha\vartheta$, and contain a flat potential, i.e. $U''(\vartheta) = 0$, are shift symmetric (D²GB and D²CS are both special cases of such theories). We can see this by locally integrating Eq. (18) by parts,

$$S_q = - \int d^4x \sqrt{-g} f'(\vartheta) (\nabla_a \vartheta) J^a + \text{bndry.}, \quad (24)$$

and noting that for the case of a linear coupling function, $f'(\vartheta) = \alpha$ is independent of ϑ . Thus a global constant shift $\vartheta \rightarrow \vartheta + c$ only changes S_q by a boundary term, so the EOMs are invariant. A shift symmetry is a natural outcome of the decoupling limit of either DCS or DGB. It may also be a desirable property built into a theory, since it protects the scalar potential from acquiring a mass via quantum corrections, since all corrections must abide by the shift symmetry.

Shift symmetry is then another feature that may be used to classify theories, which we denote as a central square in Fig. 1. D²GB and D²CS are not the only quadratic gravity theories that enjoy a shift symmetry. Another example is actions that only involve derivatives of ϑ , such as $\mathcal{L} \supset \alpha(\square\vartheta)K$. Alternatively, a theory may exhibit a discrete shift symmetry if it is periodic in ϑ , e.g. $\mathcal{L} \supset \alpha \sin(\omega\vartheta)K$, for some constant ω .

Let us comment here that TE_dGB, while not shift-symmetric, is invariant under the simultaneous field redefinition and parameter scaling $\vartheta \rightarrow \vartheta + c$, $\alpha_{\text{TEdGB}} \rightarrow \alpha_{\text{TEdGB}} e^{+\gamma c}$, for some additive constant c . Therefore we can only discuss bounds on α_{TEdGB} if we have some way of specifying the constant c . We will fix this freedom by identifying the asymptotic value ϑ_∞ .

C. Well-posedness and EFT

As presented and classified here, quadratic gravity theories may not be well-posed when treated as exact theories. The EOMs may have higher than second-order derivatives, and they may suffer from the Ostrogradski instability [90]. Indeed, [86] analyzed D²CS as an exact theory and found a problematic initial value formulation. However, not all quadratic gravity theories contain higher than second-order derivatives: DGB is the special case with only second-order EOMs.

Quadratic gravity theories should in fact be treated as *effective theories* with a limited regime of validity, rather than exact theories. This requirement comes from the expectation that GR fails as a description at some short length scale, and we may model corrections to GR in an extended regime of validity through an EFT approach [91]. Within the regime of validity of the EFT, the corrections to GR must be controllably small, so we find ourselves in the decoupling limit [e.g. Eqs. (21) and (22)]. In fact, it was shown in [86] that in the decoupling limit, D²CS is well-posed around appropriate background solutions. This same argument should hold for other higher-curvature theories when treated through order-reduction in the decoupling limit.

A common criticism here is that from dimensional analysis, the dimensional coupling coefficients³ α_X are expected to be Planck scale and thus irrelevant at astrophysical length scales. However, naive dimensional analysis seems to fail in certain sectors (most obviously in the scaling of the cosmological constant), so we will remain agnostic here. Instead, we simply parametrize our ignorance of the length scale at which GR requires corrections, and allow observations to guide theory-building.

The validity of the EFT description requires that $S_q \ll S_{\text{EH}}$ and that $S_\vartheta \ll S_{\text{EH}}$. In the geometric units used in this paper ($G = 1 = c$), the conditions for validity of the EFT in D²GB and D²CS become $\sqrt{\alpha_X} \ll (\kappa/\mathcal{C}^3)^{1/4} \mathcal{R}$ for $\alpha_X = \alpha_{\text{GB}}$ or α_{CS} , where \mathcal{R} is the radius of the smallest object in the system, and $\mathcal{C} \equiv GM/\mathcal{R}$ is its gravitational compactness (recall that in geometric units, the action has dimensions of $[S] = L^2$, thus $[\vartheta] = L^0$ is dimensionless while the coupling constant $[\alpha] = L^2$ is dimensional). The preceding scaling estimates made use of the estimate $\vartheta = \mathcal{O}[\alpha_X(\mathcal{C}/\mathcal{R})^2]$, obtained from the EOM of the scalar field. Clearly, as the dimensional coupling strength goes to zero, one recovers GR, while for sufficiently small couplings, quadratic gravity is a small deformation of Einstein's theory.

We use the fact that the theory is a small deformation of GR to establish a perturbative scheme for finding solutions in the decoupling limit [90, 92, 93]. For a more extensive discussion of this approach, see [24]. The dynamical fields—the metric, scalar field, and any other fields present—are expanded in a Taylor series. Explicitly, we have

$$\vartheta = \vartheta^{[0]} + \zeta^{1/2} \vartheta^{[1/2]} + \mathcal{O}(\zeta^1), \quad (25)$$

$$g_{ab} = g_{ab}^{[0]} + \zeta^{1/2} g_{ab}^{[1/2]} + \zeta^1 g_{ab}^{[1]} + \mathcal{O}(\zeta^{3/2}), \quad (26)$$

where ζ is a dimensionless parameter which is proportional to α_i^2 . When $\zeta \rightarrow 0$, the EOM for ϑ becomes simply $\square^{[0]}\vartheta^{[0]} = 0$ (since we are interested in long-ranged scalar fields, we have a vanishing potential). In order to satisfy asymptotic flatness, the asymptotic solution for $\vartheta^{[0]}$ must be $\lim_{r \rightarrow \infty} \vartheta^{[0]} \rightarrow \text{const}$. For the special case of a shift-symmetric theory, this latter constant can be set to zero. Then by examining the perturbed equations of motion we will find

$$\vartheta = 0 + \zeta^{1/2} \vartheta^{[1/2]} + \mathcal{O}(\zeta^{3/2}), \quad (27)$$

$$g_{ab} = g_{ab}^{[0]} + \zeta^1 g_{ab}^{[1]} + \mathcal{O}(\zeta^2). \quad (28)$$

The powers of ζ appearing above follow from setting $\vartheta^{[0]} = 0$, and the presence of the explicit α_i in the interaction term of the Lagrangian. The background that we

³ Note that one could make the replacement $\alpha_X \rightarrow \ell^2 \bar{\alpha}_X$, such that the new coupling strength is dimensionless, and all units are carried by the length scale ℓ . We will not make that choice here.

expand about is a GR solution, $g_{ab}^{[0]} = g_{ab}^{\text{GR}}$, $\vartheta^{[0]} = 0$. The most important feature of this order-reduction scheme is that order-by-order, the principle part of the differential operator acting on each $\vartheta^{[k]}$ and $g^{[k]}$ is respectively $\square^{[0]}\vartheta^{[k]}$ (the background d'Alembertian) and $G^{[1]}[g^{[k]}]$ (the linearized Einstein tensor operator). Because of this, the order-reduced EOMs are always well-posed.

D. Constraints on Quadratic Gravity Theories

Not many quadratic gravity theories have been studied in sufficient detail to be tested against observations of, for example, solar system phenomena or binary pulsars. Nevertheless, one might think that such theories have already been constrained strongly from binary pulsar observations because a theory that contains long-ranged scalar fields will predict the excitation of dipole radiation in binary systems. Such radiation would produce a much faster decay of the orbital period of binary pulsars, and since this has not been observed, such theories must already be well-constrained or ruled out.

Certain quadratic gravity theories that are shift-symmetric, however, evade this problem completely, as we will show in this paper, and thus, such theories are much less-well-constrained. The most well-studied shift-symmetric theories in the context of experimental relativity are those within the non-derivative and topological interaction class. Recall that these reduce to D²CS and D²GB in the decoupling limit. The best estimated constraint on D²GB comes from observations of low-mass X-ray binaries (LMXBs), which imply that $\sqrt{|\alpha_{\text{GB}}|} \lesssim \mathcal{O}(2 \text{ km})$ [49].⁴ The best constraint on D²CS comes from observations of frame-dragging with Gravity Probe B and the LAGEOS satellites [94] and from table-top experiments [95], which imply that $\sqrt{|\alpha_{\text{CS}}|} \lesssim \mathcal{O}(10^8 \text{ km})$.

The D²GB estimate is much stronger than the D²CS constraint for two reasons. First, the D²CS correction is only sourced by the parity-odd part of the background. Thus spherically symmetric configurations, like the exterior gravitational field of a non-rotating star, are not modified in D²CS at all, because the Pontryagin density vanishes. Secondly, there is no estimated constraint on D²CS from a stellar-mass BH system, only from the solar system. The curvature in the solar system, however, is extremely weak relative to that of BHs in LMXBs, and thus the estimated constraint on D²GB is much stronger.

III. MIRACLE HAIR LOSS THEOREM

In this section, we present a proof that asymptotically $1/r$, spherically symmetric scalar hair (which recall, we

⁴ This bound also applies to Kretschmann gravity. A similar bound is obtained on TEdGB gravity via the existence of stellar-mass BHs [50, 51].

refer to in this paper as the *scalar charge*) cannot be supported by objects with no event horizon, like NSs and ordinary stars, in the decoupling limit of Gauss-Bonnet gravity. This proof both generalizes and makes more rigorous the ‘‘physicist’s proof’’ presented in [24], but it follows the same spirit. We first state the theorem and then give a sketch of the proof, which we hope is convincing to most readers. We then present a complete proof for those readers desiring more mathematical rigor.

Theorem 1. *Consider a 4-dimensional manifold M which is homeomorphic to Minkowski (thus excluding black hole spacetimes, which are ‘punctured’). Let M be endowed with a metric g with Lorentz signature, which is stationary and asymptotically flat [96, 97]. We require that the Riemann curvature tensor is continuous almost everywhere,⁵ with any discontinuities in a spatially compact set of measure zero. We also require that, in an asymptotically Cartesian coordinate system, the components of the Riemann tensor decay at least as $\mathcal{O}(r^{-2})$.⁶ Further, consider a real scalar field ϑ , stationary under the same isometry as the metric, whose dynamics are governed by a linear coupling in the action to the Gauss-Bonnet density, thus satisfying an EOM*

$$\square\vartheta = c_1 (*R_{abcd} *R^{cdab}) \quad (29)$$

for some constant real number c_1 . Then the asymptotically $1/r$, spherically-symmetric scalar hair (the scalar charge) vanishes.

Sketch of the proof. Our proof begins by integrating the EOMs [Eq. (29)] over a suitably chosen spacetime region C ,

$$\int_C \square\vartheta \sqrt{-g} d^4x = c_1 \int_C *R *R \sqrt{-g} d^4x. \quad (30)$$

As depicted in Fig. 2, the region C is a spatial 3-ball crossed with a segment of time, $t \in [0, T]$. For technical reasons, we compactify the time direction $t \sim t+T$, which for a stationary situation does not change the physics.

We now manipulate the right-hand side of Eq. (30). First, we use the generalized Gauss-Bonnet-Chern (GBC) theorem for (pseudo-)Riemannian manifolds [98, 99] with boundary [100, 101]. This converts the integral into a sum of (i) a topological number that vanishes for our topology, and (ii) a boundary integral. Thus we have

$$\int_C \square\vartheta \sqrt{-g} d^4x = -c_2 \oint_{\partial C} \Theta(\mathbf{n}), \quad (31)$$

⁵ In the sense of measure theory, a property holds *almost everywhere* if the set of points where it fails to hold has measure zero. Curvature tensors may be discontinuous for a body with a solid surface where the density goes to zero discontinuously; e.g. in GR, the Ricci tensor is nonzero inside the body but it vanishes outside, with a discontinuity at the surface.

⁶ To establish the Riemann-integrability of the Gauss-Bonnet density, we need the discontinuities to have measure-zero, and for Riemann to have sufficiently fast asymptotic fall-off.

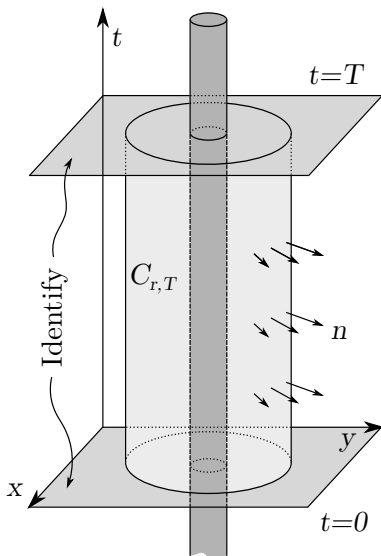


FIG. 2. Spacetime geometry for our proof. Time t is up, two spatial dimensions are presented as x, y and one spatial dimension is suppressed. The dark shaded cylinder represents the world tube of the compact matter sources, e.g. a stationary isolated neutron star. The integration region is the lighter shaded cylinder $C_{r,T}$, a spatial 3-ball of radius r over the time interval $t \in [0, T]$. We compactify the time axis by the identification $t \sim t + T$, giving our time axis the topology of a circle S^1 . The region $C_{r,T}$ has unit outward normal vector \mathbf{n} .

where $\Theta(\mathbf{n})$ is a 3-form which depends on the outward spatial unit normal vector \mathbf{n} , and c_2 is another constant multiple of c_1 . The integral of the right-hand side at large radius r exists and decays at least as r^{-1} .

Next we manipulate the left-hand side of Eq. (30). First, we use the generalized Stokes theorem to convert the integral to another boundary integral, and consider the limit as $r \rightarrow \infty$:

$$\lim_{r \rightarrow \infty} T \oint_{\partial C} (\partial_r \vartheta) r^2 d^2 \Omega = 0, \quad (32)$$

where $d^2 \Omega = \sin \theta d\theta d\phi$ is the area element on the unit 2-sphere. In the limit as $r \rightarrow \infty$, this integral exists and depends on only the scalar charge μ , which recall we define as

$$\vartheta = \frac{\mu}{r} + \mathcal{O}(r^{-2}). \quad (33)$$

Thus, we find

$$4\pi T \mu = 0,$$

which implies that $\mu = 0$. \square

The sketch presented above summarizes the proof that scalar charge cannot be supported by objects without event horizons in a quadratic gravity theory in which the scalar field satisfies Eq. (29). In particular, this is the case in the decoupling limit of dynamical Gauss-Bonnet

gravity, i.e. in D²GB where $c_1 = \alpha_{\text{GB}}$. Those readers who are satisfied with this level of detail may proceed to the next Section. For those desiring mathematical rigor, we now present the complete proof.

Proof. Our proof makes use of a special case of the generalized Gauss-Bonnet-Chern theorem for manifolds with boundary and indefinite metric, presented by Alty [100] and later by Gilkey and Park [101]. Let us briefly restate this theorem for the special case of a 4-dimensional manifold \mathcal{M} with metric g of signature $(-+++)$ or $(+---)$. Let \mathcal{M} have a (potentially empty) boundary $\partial\mathcal{M}$ with an induced metric on each of its connected components whose signature never changes sign, i.e. each component has a normal \mathbf{n} which is either everywhere spacelike, everywhere timelike, or everywhere null. Then, the 4-dimensional generalized Gauss-Bonnet-Chern theorem says that⁷

$$\chi(\mathcal{M}) = (-1)^{[p/2]} \left[\int_{\mathcal{M}} \Delta + \int_{\partial\mathcal{M}} \Theta(\mathbf{n}) \right], \quad (34)$$

where $\chi(\mathcal{M})$ is the Euler characteristic of \mathcal{M} and $[p/2]$ is the largest integer $\leq p/2$. The 4-form Δ is given by [100]

$$\Delta = \frac{1}{128\pi^2} \epsilon_{abcd} \epsilon^{a'b'c'd'} R^{ab}{}_{a'b'} R^{cd}{}_{c'd'} \sqrt{-g} d^4 x, \quad (35)$$

and the 3-form $\Theta(\mathbf{n})$ is given by [100]

$$\Theta(\mathbf{n}) = [\Theta_1(\mathbf{n}) - \Theta_2(\mathbf{n})] {}^{(3)}\epsilon(\mathbf{n}), \quad (36)$$

$$\Theta_1(\mathbf{n}) = \frac{1}{16\pi^2} {}^{(3)}\epsilon_{abc} {}^{(3)}\epsilon^{a'b'c'} R^{ab}{}_{a'b'} n^c{}_{;c'}, \quad (37)$$

$$\Theta_2(\mathbf{n}) = \frac{1}{12\pi^2} {}^{(3)}\epsilon_{abc} {}^{(3)}\epsilon^{a'b'c'} n^a{}_{;a'} n^b{}_{;b'} n^c{}_{;c'}, \quad (38)$$

with ${}^{(3)}\epsilon_{abc} = n^d \epsilon_{dabc}$ the induced volume 3-form in the tangent subspace orthogonal to \mathbf{n} .

To apply the 4-dimensional generalized Gauss-Bonnet-Chern theorem, we will take the manifold $\mathcal{M} \equiv C'_{r,T}$ to be a submanifold $C'_{r,T} \subset M$ of the whole spacetime. We start with a submanifold $C_{r,T}$ which is a spatial 3-ball B_r of radius r crossed with a time interval $t \in [0, T]$. This submanifold does not satisfy the conditions of Alty's proof because (i) the boundary is not smooth, having "corners" at the ends of the 4-cylinder (see Fig. 2), and (ii) the boundary $\partial C_{r,T}$ has a normal which is timelike in some regions (the top/bottom of the 4-cylinder) and spacelike in others (the sides of the 4-cylinder). However, because the spacetime is stationary, the physics is not affected by compactifying the time direction. Thus, we

⁷ The careful reader will note that Alty's theorem was more general, allowing for vector fields other than \mathbf{n} . The price for this generalization is to also include the topological *kink* number [100], which vanishes when only considering \mathbf{n} ; hence we omit it. Gilkey and Park [101] make this same simplification, also omitting the kink number.

use the identification $t \sim t+T$, which turns the time axis from \mathbb{R} into S^1 . This glues the top and bottom of the 4-cylinder together, giving it the topology of $B_r \times S^1$. We call this glued manifold $C'_{r,T}$. The boundary $\partial C'_{r,T}$ has topology $S^2 \times S^1$, and the normal is everywhere spacelike, satisfying the conditions to apply Alty's proof.

We now proceed by integrating the EOMs [Eq. (29)] over the region $C'_{r,T}$,

$$\int_{C'_{r,T}} \square \vartheta \sqrt{-g} d^4 x = c_1 \int_{C'_{r,T}} (*R_{abcd} *R^{cdab}) \sqrt{-g} d^4 x. \quad (39)$$

First we investigate the right-hand side, and apply Eq. (34), which gives

$$\int_{C'_{r,T}} \square \vartheta \sqrt{-g} d^4 x = c_2 \left[\chi(C'_{r,T}) - \int_{\partial C'_{r,T}} \Theta(\mathbf{n}) \right], \quad (40)$$

in the case of $p = 1$ (the final result is the same for $p = 3$), where $c_2 = 32\pi^2 c_1$. The Euler characteristic of a product manifold satisfies $\chi(M \times N) = \chi(M) \cdot \chi(N)$, and $\chi(S^1) = 0$, thus $\chi(C'_{r,T}) = 0$. Thus, we have

$$\int_{C'_{r,T}} \square \vartheta \sqrt{-g} d^4 x = -c_2 \int_{\partial C'_{r,T}} \Theta(\mathbf{n}). \quad (41)$$

We now must prove that in the limit $r \rightarrow \infty$, each side of Eq. (41) exists (i.e. both integrals converge). We start with the asymptotic behavior of the integrand $\Theta(\mathbf{n})$. In a stationary, asymptotically flat spacetime [96, 97], in asymptotically Cartesian coordinates (t, x, y, z) , the metric has asymptotic fall-off

$$g_{ab} = \eta_{ab} + \mathcal{O}(r^{-1}), \quad (42)$$

with r defined in the ordinary Cartesian fashion, $r^2 = x^2 + y^2 + z^2$. It is this function that defines the region $C'_{r,T}$, and thus, $n_a = \nabla_a r$. In these same coordinates, the behavior of $n^a{}_{;b}$ is

$$n^a{}_{;b} = r^{-1}(\delta_b^a - n^a n_b) + \mathcal{O}(r^{-2}). \quad (43)$$

By assumption, we also have the asymptotic fall-off for the components of the Riemann tensor, in an asymptotically Cartesian coordinate system, $R_{abcd} \sim \mathcal{O}(r^{-2})$ [true for all index positions because of Eq. (42)]. In fact, Eq. (42) implies $R_{abcd} \sim \mathcal{O}(r^{-3})$, but only the weaker condition $\mathcal{O}(r^{-2})$ is required for our proof.

Now we can see the leading asymptotic behavior of the integrands on the right-hand side of Eq. (41):

$$\Theta_1(\mathbf{n}) \sim \mathcal{O}(r^{-3}), \quad (44)$$

$$\Theta_2(\mathbf{n}) \sim \mathcal{O}(r^{-3}). \quad (45)$$

Actually, $\Theta_1(\mathbf{n})$ decays as $\mathcal{O}(r^{-4})$ following the fall-off of Riemann determined by Eq. (42), but again we only need the weaker decay. When integrated over $\partial C'_{r,T}$, we find that the integral exists and converges at least as

$$\int_{\partial C'_{r,T}} \Theta(\mathbf{n}) \sim \mathcal{O}(r^{-1}), \quad (46)$$

and in the limit as $r \rightarrow \infty$,

$$\lim_{r \rightarrow \infty} \int_{\partial C'_{r,T}} \Theta(\mathbf{n}) = 0. \quad (47)$$

We now turn to the left-hand side of Eq. (41), where we can apply the generalized Stokes theorem to turn the volume integral into a boundary integral:

$$\int_{C'_{r,T}} \square \vartheta \sqrt{-g} d^4 x = \int_{\partial C'_{r,T}} d\Sigma_a \nabla^a \vartheta, \quad (48)$$

where $d\Sigma_a$ is the area element on the boundary $\partial C'_{r,T}$. In asymptotically spherical coordinates, this is given by

$$d\Sigma_r = r^2 d^2 \Omega dt [1 + \mathcal{O}(r^{-1})], \quad (49)$$

where the standard unit 2-sphere area element is $d^2 \Omega = \sin \theta d\theta d\phi$, and other components of $d\Sigma_a$ are subdominant and vanish in the limit $r \rightarrow \infty$. To show convergence we must study the behavior of asymptotic solutions to Eq. (29).

The solution for ϑ will be a combination of homogeneous and particular solutions, $\vartheta = \vartheta_{\text{hom}} + \vartheta_{\text{part}}$, subject to the condition of asymptotic flatness. Let us first consider the homogeneous solution. In the limit $r \rightarrow \infty$, Eq. (29) reduces to the flat-space Laplacian (from stationarity and asymptotic flatness); thus we know that

$$\vartheta_{\text{hom}} \sim \sum_{lm} Y_{lm}(\theta, \phi) \left[\frac{a_{lm}}{r^{l+1}} + b_{lm} r^l \right], \quad (50)$$

for coefficients a_{lm}, b_{lm} . To satisfy asymptotic flatness as $r \rightarrow \infty$, we must have $b_{lm} = 0$ except for b_{00} . The coefficient b_{00} is determined by boundary conditions (or, in the case of a shift-symmetric theory, it can be set to any value). The integral in Eq. (48) is insensitive to b_{00} since only the derivative $\nabla_a \vartheta$ enters the integrand.

We now consider the particular solution. The non-compact source term, $*R *R$, decays at least as $\mathcal{O}(r^{-4})$ [in fact as $\mathcal{O}(r^{-6})$ following Eq. (42), but again we only need the weaker decay]. Therefore, the slowest-decaying contribution from the particular solution is at worst

$$\vartheta_{\text{part}} \sim r^{-2} \quad \text{or} \quad r^{-2} \log r. \quad (51)$$

This log term arises if there is an r^{-4} component in the $l = 1$ term of the spherical harmonic decomposition of the source term, $*R *R$.

Now we can show that the left-hand side integral of Eq. (41) converges. From asymptotic flatness and in asymptotically spherical coordinates we have

$$\lim_{r \rightarrow \infty} \int_{\partial C'_{r,T}} d\Sigma^a \nabla_a \vartheta = \lim_{r \rightarrow \infty} \int_{\partial C'_{r,T}} dt d^2 \Omega r^2 \partial_r \vartheta. \quad (52)$$

With the far-field asymptotic behavior of ϑ_{hom} and ϑ_{part} given in Eqs. (50) and (51), the only part of $\partial_r \vartheta$ that contributes is

$$\partial_r \vartheta = \partial_r (\vartheta_{\text{hom}} + \vartheta_{\text{part}}) = -\frac{a_{00}}{r^2} [1 + \mathcal{O}(r^{-1})]. \quad (53)$$

	α_1	α_2	α_3	α_4	$g(\vartheta)$
Kretsch. gravity	0	0	α_K	0	ϑ
TEdGB gravity	α_{TEdGB}	$-4\alpha_{\text{TEdGB}}$	α_{TEdGB}	0	$e^{-\gamma\vartheta}$
D ² GB gravity	α_{GB}	$-4\alpha_{\text{GB}}$	α_{GB}	0	ϑ

TABLE II. Parameter mapping for non-derivative, quadratic gravity theories that we investigate in detail.

We conventionally call $a_{00} = \mu$ the scalar charge [compare for example with Eq. (33)]. Thus, the left-hand side converges to

$$\lim_{r \rightarrow \infty} \int_{\partial C'_{r,T}} d\Sigma^a \nabla_a \vartheta = -4\pi T \mu. \quad (54)$$

We have now shown that the integrals on both the left- and the right-hand sides converge in the limit $r \rightarrow \infty$. Inserting the limits [Eq. (47) and Eq. (54)] into the volume-integrated equation of motion [Eq. (41), after applying the GBC theorem] yields

$$4\pi T \mu = 0. \quad (55)$$

Thus we have proved that the asymptotically $1/r$, spherically-symmetric scalar charge μ must vanish. \square

IV. NEUTRON STAR SCALAR CHARGE IN QUADRATIC GRAVITY

In this section, we derive the NS scalar charge in a few quadratic gravity theories. In particular, we focus on theories with non-derivative interactions but allow for both topological and non-topological interaction densities (the bottom rectangle in Fig. 1). Such theories are defined through the interaction density of Eq. (9), which with a certain choice for $f_i(\vartheta)$, leads to the quadratic action

$$S_q = \int d^4x \sqrt{-g} g(\vartheta) [\alpha_1 R^2 + \alpha_2 R_{ab} R^{ab} + \alpha_3 R_{abcd} R^{abcd} + \alpha_4 {}^* R_{abcd} R^{abcd}], \quad (56)$$

where $(\alpha_1, \alpha_2, \alpha_3, \alpha_4)$ are all constants. This particular choice of $f_i(\vartheta)$ allows us to recover the examples discussed in Sec. II through appropriate choices of $g(\vartheta)$, as shown in Table II. Notice also that D²GB gravity can be recovered from TEdGB gravity by taking the limit $\gamma \rightarrow 0$ while $\gamma \alpha_{\text{TEdGB}} \rightarrow -\alpha_{\text{GB}} = \text{const.}$

The NS scalar charge is obtained by solving the EOM for the scalar field. The latter follows from Eq. (8), which with a vanishing potential ($U = 0$) and the non-derivative, quadratic gravity action of Eq. (56) reduces to $\square\vartheta = S$, where we have defined the source function

$$S \equiv - \left(\frac{\partial g}{\partial \vartheta} \right) (\alpha_1 R^2 + \alpha_2 R_{ab} R^{ab} + \alpha_3 R_{abcd} R^{abcd} + \alpha_4 {}^* R_{abcd} R^{abcd}). \quad (57)$$

Once we solve the EOM and extract the scalar charge, we will use it in the next Section to determine the best systems to constrain such theories, and estimate new constraints when possible.

We first concentrate on deriving the scalar charge of a non-rotating NS, and then extend the analysis to a rotating configuration. In each case, we will first calculate the scalar charge analytically within a weak-field approximation scheme and for certain simple equations of state. We will then confirm our results numerically in the strong-field regime and for more complicated equations of state. We will explicitly demonstrate the vanishing of the scalar charge in D²GB gravity, which was proven formally in the previous section, and also show that the scalar charge does not vanish in TEdGB gravity or in Kretschmann gravity.

For the purposes of comparison, we note here that the scalar charge has also been computed for BHs in several quadratic gravity theories [24, 30–33, 50, 102]. In the decoupling limit of any non-derivative quadratic gravity theory, for a BH with a mass M_{BH} and at leading order in spin, the dimensionless (mass-reduced) scalar charge is given by

$$\mu_{\text{BH}}^{(0)} = 2g'(0) \frac{\alpha_3}{M_{\text{BH}}^2}. \quad (58)$$

This is non-vanishing for D²GB, to be compared with the vanishing of scalar charge for NSs.

A. Non-rotating Neutron Stars

Let us first consider a non-rotating stellar configuration, described by a perfect fluid matter source that generates a spherically symmetric spacetime. Given this, the scalar field can only be a function of the radial coordinate, namely $\vartheta = \vartheta^{(0)}(r)$. The superscript (0) reminds us that we can think of $\vartheta^{(0)}$ as the zeroth-order term in a small-spin expansion. The GR metric is then simply

$$ds_{(0)}^2 = -e^\nu dt^2 + \left(1 - \frac{2M}{r}\right)^{-1} dr^2 + r^2 (d\theta^2 + \sin^2 \theta d\varphi^2), \quad (59)$$

where $M = M(r)$ is the spherically-symmetric enclosed mass and $\nu = \nu(r)$ is a metric function that satisfies the Einstein equations. The scalar field evolution equation is then

$$\frac{d^2 \vartheta^{(0)}}{dr^2} = - \frac{2[2\pi(p - \rho)r^3 + r - M]}{r(r - 2M)} \frac{d\vartheta^{(0)}}{dr} + S^{(0)}, \quad (60)$$

where $p(r)$ and $\rho(r)$ are the internal pressure and energy density, and $S^{(0)}$ is the function evaluated on $g_{ab}^{(0)}$ [see Eq. (A1)]. The calculation of the scalar charge requires that we first solve Eq. (60) inside the star and then

match it to an exterior solution at the stellar surface to determine any constants of integrations.

Analytic solutions to Eq. (60) for the scalar field do not generically exist in closed-form, but they can be obtained using certain approximations, such as a *post-Minkowskian* or *weak-field* expansion. In a post-Minkowskian expansion, one expands and solves the equations in powers of the compactness $C = M_*/R_* \ll 1$, where M_* and R_* are the NS mass and radius.⁸ But even with such an approximation, Eq. (60) can still only be solved for certain particular equations of state [103–105]. We focus here on an $n = 0$ polytropic equation of state [103] ($p = K\rho^{1+1/n}$, where K and n are constants with the latter representing the polytropic index) and a Tolman VII equation of state [104, 105] with $\rho \propto 1 - r^2/R_*^2$. These represent a constant density star and an approximation to more realistic equations of state respectively.

Given the above, we compute the scalar charge as follows. First, we substitute the analytic, GR solutions⁹ to the equations of structure for the metric tensor and pressure at zeroth-order in rotation into Eq. (60). We next substitute Eq. (27) in Eq. (60) and expand the equation order by order in ζ . The exterior solutions can be obtained by setting $p = 0 = \rho$, $M = M_*$ and solving the decomposed equations order by order, as given by Eqs. (A3) and (A4). Meanwhile, the interior solutions can be obtained as a further expansion in powers of C . We match these exterior and interior solutions order by order in C and ζ at the stellar surface using the condition given by Eq. (A16).

Once a solution to Eq. (60) has been obtained, we can then read off the $1/r$ piece of the external solution and calculate

$$\vartheta_{\text{ext}}^{(0)}(r) = \vartheta_\infty + \mu^{(0)} \frac{M_*}{r} + \mathcal{O}\left(\frac{M_*^2}{r^2}\right) \quad (61)$$

far from the source ($r \gg M_*$). Here, $\mu^{(0)}$ is the dimensionless scalar charge at zeroth-order in spin and ϑ_∞ is a constant that the scalar field asymptotes to at spatial infinity. Recall again that this constant can be set to zero in theories that are shift symmetric.

Let us now present the scalar charge in TEdGB, D²GB and Kretschmann gravity. In order to reveal whether and how the scalar charge vanishes, let us consider the theory defined by the interaction density of Eq. (56) with

$$g(\vartheta) = e^{-\gamma\vartheta}, \quad (62)$$

and $\alpha_4 = 0$. We recover the theories mentioned above by taking the following limits

- *TEdGB limit*: $(\alpha_1, \alpha_2, \alpha_3) \rightarrow \alpha_{\text{TEdGB}}(1, -4, 1)$.
- *Kretschmann limit*: $\gamma \rightarrow 0$, while $\gamma(\alpha_1, \alpha_2, \alpha_3) \rightarrow -\alpha_{\text{K}}(0, 0, 1)$ for a constant α_{K} .
- *D²GB limit*: $\gamma \rightarrow 0$, while $\gamma(\alpha_1, \alpha_2, \alpha_3) \rightarrow -\alpha_{\text{GB}}(1, -4, 1)$ for a constant α_{GB} .

With this in mind, the scalar charge for a NS with an $n = 0$ polytropic equation of state is

$$\begin{aligned} \mu_{n=0}^{(0)} = & -12 \gamma e^{-\gamma\vartheta_\infty} \frac{C}{R_*^2} \left(\alpha_{\text{GB},1} - \frac{3}{5} \alpha_{\text{GB},2} C - \frac{18}{35} \alpha_{\text{GB},2} C^2 \right) \\ & - \frac{96}{35} \gamma^3 e^{-2\gamma\vartheta_\infty} \frac{C^3}{R_*^4} \left[32\alpha_3^2 + 63\alpha_{\text{GB},2}(\alpha_{\text{GB},2} - \alpha_3) \right] \\ & + \mathcal{O}\left(\zeta^{3/2}, C^4\right), \end{aligned} \quad (63)$$

while for a Tolman VII equation of state we find

$$\begin{aligned} \mu_{\text{Tol}}^{(0)} = & -\frac{120}{7} \gamma e^{-\gamma\vartheta_\infty} \frac{C}{R_*^2} \left[\alpha_{\text{GB},2} - \frac{1}{22} (19\alpha_{\text{GB},1} + \alpha_{\text{GB},2}) C \right. \\ & \left. - \frac{1}{2145} (1583\alpha_{\text{GB},1} + 177\alpha_{\text{GB},2}) C^2 \right] \\ & - \frac{320}{1001} \gamma^3 e^{-2\gamma\vartheta_\infty} \frac{C^3}{R_*^4} \left[1008\alpha_3^2 + 5\alpha_{\text{GB},2} (300\alpha_{\text{GB},2} \right. \\ & \left. - 373\alpha_3) \right] + \mathcal{O}\left(\zeta^{3/2}, C^4\right), \end{aligned} \quad (64)$$

where we have here defined

$$\alpha_{\text{GB},1} \equiv 3\alpha_1 + \alpha_2 + \alpha_3, \quad \alpha_{\text{GB},2} \equiv \alpha_1 + \alpha_2 + 3\alpha_3. \quad (65)$$

Both combinations $\alpha_{\text{GB},1}, \alpha_{\text{GB},2}$ vanish for the Gauss-Bonnet ratio $(\alpha_1, \alpha_2, \alpha_3) \propto (1, -4, 1)$. Note that the terms proportional to R_*^{-2} and R_*^{-4} in Eqs. (63) and (64) are of $\mathcal{O}(\zeta^{1/2})$ and $\mathcal{O}(\zeta)$ respectively.

Let us now take the aforementioned limits to investigate the scalar charge in TEdGB, D²GB and Kretschmann gravity. In the Kretschmann limit, Eqs. (63) and (64) reduce to

$$\begin{aligned} \mu_{n=0}^{(0),\text{K}} = & 12\alpha_{\text{K}} \frac{C}{R_*^2} \left(1 - \frac{9}{5} C - \frac{54}{35} C^2 \right) + \mathcal{O}\left(\zeta^{3/2}, C^4\right), \quad (66) \\ \mu_{\text{Tol}}^{(0),\text{K}} = & \frac{360}{7} \alpha_{\text{K}} \frac{C}{R_*^2} \left(1 - \frac{1}{3} C - \frac{2114}{6435} C^2 \right) + \mathcal{O}\left(\zeta^{3/2}, C^4\right). \quad (67) \end{aligned}$$

Observe that the $\mathcal{O}(\zeta)$ contribution vanishes in Kretschmann gravity because the scalar field is linearly coupled to the Kretschmann density in the quadratic action. In fact, the $\mathcal{O}(\zeta)$ part of the scalar charge vanishes generically for any quadratic gravity where the scalar field is coupled *linearly* to a quadratic curvature scalar, i.e. for any non-derivative quadratic gravity theory to leading-order in the decoupling limit.

⁸ Neutron stars are objects with small compactness, typically of $\mathcal{O}(10^{-1})$, so a post-Minkowskian expansion is well-justified.

⁹ The effect of non-GR corrections to the metric on the scalar charge can be neglected to the order we work on, as explained in App. A 1 a.

Next, let us investigate the TEdGB limit. Since in this limit $\alpha_{\text{GB},1,2} \rightarrow 0$, the scalar charge becomes

$$\mu_{n=0}^{(0),\text{TEdGB}} = -\frac{3072}{35} \gamma^3 e^{-2\gamma\vartheta_\infty} \alpha_{\text{TEdGB}}^2 \frac{C^3}{R_*^4} + \mathcal{O}(\zeta^{3/2}, C^4), \quad (68)$$

$$\mu_{\text{Tot}}^{(0),\text{TEdGB}} = -\frac{46080}{143} \gamma^3 e^{-2\gamma\vartheta_\infty} \alpha_{\text{TEdGB}}^2 \frac{C^3}{R_*^4} + \mathcal{O}(\zeta^{3/2}, C^4). \quad (69)$$

Notice that the $\mathcal{O}(\zeta^{1/2})$ contribution vanishes in this case and the leading order contribution is of $\mathcal{O}(\zeta)$. Such a modification would be of *second-order* in the coupling constants, and thus, a consistent treatment would require inclusion of terms of the same order in the non-minimal curvature coupling at the level of the action—we ignore such terms here, although in principle they could cancel the above result. Notice also that the leading-order terms are proportional to C^3 , whereas those in Eqs. (63) and (64) are proportional to C . Therefore, the scalar charges in TEdGB gravity are quadratically suppressed by the stellar compactness. We have checked that these analytic results match the purely numerical calculation of [106].

Finally, let us now consider the D²GB limit. We can do this by simply taking the $\gamma \rightarrow 0$ limit of Eqs. (68) and (69) while $\gamma\alpha_{\text{TEdGB}}$ remains finite. Doing so, one finds that the scalar charge vanishes identically to $\mathcal{O}(\zeta)$. From the $\mathcal{O}(\zeta^{1/2})$ contribution in Eqs. (63) and (64), one sees that the Gauss-Bonnet combination is the only one that can make the scalar charge vanish. Moreover, the charge depends on different combinations of $\alpha_{\text{GB},1,2}$ at different orders in compactness, but in all cases, the charge vanishes linearly with $\alpha_{\text{GB},1}$ and $\alpha_{\text{GB},2}$ in the Gauss-Bonnet limit.

Given the result of Sec. III, we know that this vanishing must hold to all orders in compactness. We can further support this expectation with another explicit analytic example, without imposing a post-Minkowskian expansion. Determining this in closed-form is difficult in general, but doable for strongly *anisotropic* NSs with an $n = 0$ polytropic equation of state. Let us then consider anisotropic NSs following [107] as a *toy model*, which allows for solutions to the equations of stellar structure analytically without any approximations. We consider the strongly anisotropic limit, in which the radial pressure vanishes, so that calculations are analytically tractable. Working in D²GB gravity, we solve the scalar field equation in the interior region analytically without a post-Minkowskian expansion, then match the solution to the exterior one at the surface and find that the scalar charge vanishes exactly (see App. A3 for more detailed calculations).

We can also show that the scalar charge vanishes in D²GB gravity for more general equations of state and isotropic matter, provided we carry out a numerical analysis. Details of the numerical algorithm are explained

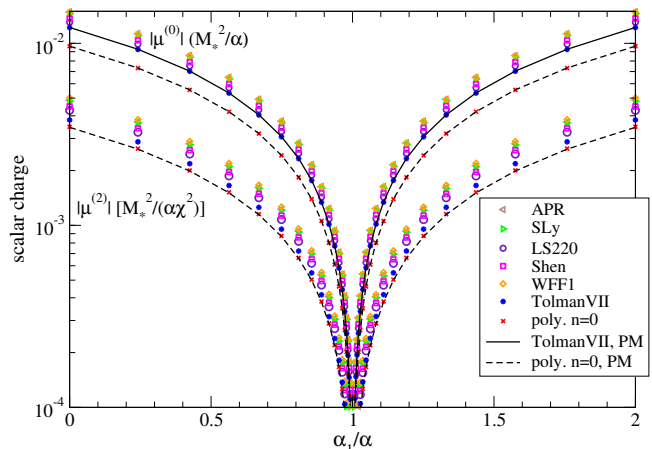


FIG. 3. (Color online) Scalar monopole charge in non-derivative, quadratic gravity in the decoupling limit for various equations of state at zeroth- ($\mu^{(0)}$) and second-order ($\mu^{(2)}$) in rotation as a function of α_1/α with α an arbitrary constant. For this example, we set $C = 0.1$, $\alpha_2 = -4\alpha$ and $\alpha_3 = \alpha$. For the TolmanVII stars and the $n = 0$ polytropes, we further set $R_* = 12$ km. Observe that the charges approach zero rapidly as one approaches the Gauss-Bonnet limit ($\alpha_1/\alpha \rightarrow 1$). Solid and dashed curves represent the analytic relation for the TolmanVII models and the $n = 0$ polytropes within the PM approximation.

in App. A2. As an example, let us consider the non-derivative, quadratic gravity model of Eq. (56) in the decoupling limit, i.e. with $g(\vartheta) = \vartheta$. Such a model contains both D²GB gravity and Kretschmann gravity, as one can see in Table II. Figure 3 shows the scalar charge for NSs with $\alpha_2 = -4\alpha$, $\alpha_3 = \alpha$ and $C = 0.1$. Observe how the charge vanishes as the Gauss-Bonnet limit ($\alpha_1/\alpha \rightarrow 1$) is approached for all equations of state considered. For comparison, we also include the scalar charge computed for an $n = 0$ polytrope and a Tolman VII equation of state numerically (red crosses and blue circles) and in a post-Minkowskian expansion (dashed and solid curves). Observe how good of an approximation the post-Minkowskian expansion is relative to the numerical solutions.

B. Slowly-rotating Neutron Stars

The theorem in Sec. III is not only more rigorous than that presented in Ref. [24], but it can also be applied to a rotating NS. We here explicitly demonstrate that the scalar charge vanishes in D²GB gravity even for a slowly-rotating configuration both analytically and numerically. To do so, we consider a quadratic gravity theory with the quadratic action of Eq. (56) but with a linear coupling function $g(\vartheta) = \vartheta$. This will allow us to investigate how the scalar charge vanishes in the D²GB limit.

We work in a slow-rotation expansion of Hartle and Thorne [108, 109] to quadratic order in spin, i.e. a sys-

tematic expansion in $J/M_*^2 \ll 1$, where $J \equiv |\vec{J}|$ is the magnitude of the spin angular momentum. Physically, we assume that $M_*\Omega \ll 1$, or equivalently $M_*/P \ll 1$, where Ω and P are the spin angular frequency and spin period of the star respectively. Such an assumption is well-justified for all observed pulsars, even those with millisecond periods for which $M_*\Omega = \mathcal{O}(10^{-2})$.

Because non-rotating stars are spherically symmetric, deformations due to rotation can be modeled through a spherical harmonic decomposition. The scalar field can then be decomposed as

$$\vartheta(r, \theta) = \vartheta^{(0)}(r) + \sum_{l=0,2} \vartheta_l^{(2)}(r) P_l(\cos \theta) + \mathcal{O}[(M_*\Omega)^4], \quad (70)$$

where r and θ are radial¹⁰ and polar coordinates respectively, $P_l(\cdot)$ are Legendre polynomials, and $\vartheta_\ell^{(2)} = \mathcal{O}[(M_*\Omega)^2]$. As expected, there is no azimuthal angle dependence, because rotating stars remain axisymmetric when in slow rotation.

The scalar charge is the piece of the scalar field that decays as $1/r$ at spatial infinity and is independent of θ , and thus, we must solve for $\vartheta^{(0)}$ and $\vartheta_0^{(2)}$. The former leads to the scalar charge in spherical symmetry, which we already considered in the previous subsection, so we here concentrate on the spin-dependent correction to the scalar charge found in $\vartheta_0^{(2)}$. One can define the dimensionless scalar charge $\mu^{(2)}$ at quadratic order in spin from the asymptotic behavior of $\vartheta_0^{(2)}$ at spatial infinity in the same way as in Eq. (61):

$$\vartheta_{0,\text{ext}}^{(2)}(r) = \mu^{(2)} \frac{M_*}{r} + \mathcal{O}\left(\frac{M_*^2}{r^2}\right). \quad (71)$$

Here, we set $\vartheta_{0,\text{ext}}^{(2)}(\infty) = 0$ without loss of generality by absorbing it into ϑ_∞ . As mentioned earlier, we uniquely specify ϑ_∞ to be a constant (which we will set to 0 in Sec. VC) to all orders in rotation in order to fix the freedom of simultaneous redefinition of α_{TEdGB} and ϑ ; fixing this freedom is required to discuss limits on α_{TEdGB} . The field equation for $\vartheta_0^{(2)}$ has the same form as Eq. (60), except that $S^{(0)}$ needs to be replaced by $S^{(2)}$, whose explicit form with a linear coupling function is given in Eq. (A10). As in the non-rotating case, we work in the small coupling approximation by decomposing $\vartheta_l^{(2)}$ in terms of $\zeta^{1/2}$ and solving the decomposed field equation order by order. The exterior solution for the scalar field at second order in spin and to leading order in $\zeta^{1/2}$ is given by Eq. (A11).

We now derive $\mu^{(2)}$ analytically within the post-Minkowskian approximation. As in the non-rotating

case, we expand the scalar field equation at second order in spin about $C = 0$ and solve it order by order in C in the interior region. We then match this solution to the exterior solution expanded in $C \ll 1$, using the conditions in Eqs. (A17) and (A18). With an $n = 0$ polytropic equation of state, we find

$$\begin{aligned} \mu_{n=0}^{(2)} = 12\Omega^2 & \left[\alpha_{\text{GB},1} - \frac{1}{20} (12\alpha_{\text{GB},1} + 61\alpha_{\text{GB},2}) C \right. \\ & \left. + \frac{3}{7} \left(\frac{13}{4}\alpha_{\text{GB},1} - \frac{9}{25}\alpha_{\text{GB},2} \right) C^2 \right] + \mathcal{O}\left(\zeta^{3/2}, C^3\right). \end{aligned} \quad (72)$$

Notice that $\mu_{n=0}^{(2)}$ vanishes to $\mathcal{O}(\zeta)$ in the D²GB limit, i.e. when $\alpha_{\text{GB},1,2} \rightarrow 0$, in agreement with Sec. III. We do not present $\mu^{(2)}$ with a TolmanVII equation of state because then we can only solve the equations of structure analytically at zeroth order in rotation.

We next carry out a numerical calculation without imposing the post-Minkowskian approximation and for a variety of realistic equations of state. We use the same numerical algorithm presented in App. A2. The results of this numerical investigation for non-derivative, quadratic gravity in the decoupling limit are presented in Fig. 3. Observe how $\mu^{(2)}$ approaches zero as one approaches the D²GB limit, just like $\mu^{(0)}$ does. Observe also that the numerical results for an $n = 0$ polytrope agree very well with the analytic ones in Eq. (72).

V. CURRENT AND FUTURE CONSTRAINTS

In this section, we study what estimated and projected constraints can be placed on some of the quadratic gravity theories discussed in Sec. II, using binary pulsar observations and GW observations. We begin in Sec. VA with a discussion of how a non-vanishing scalar charge leads to the emission of dipolar radiation, which affects the orbital period decay of binary systems and the gravitational waves they emit.

Consider a binary system emitting dipolar radiation at the orbital period. If the system is observed via pulsar timing, the leading deviation from GR is the correction to the post-Keplerian parameter \dot{P}_b , the binary's period derivative. This correction enters at -1PN relative to the GR effect. Meanwhile if the system is observed through GWs, the deformation from the GR GW prediction can be captured via the β_{ppE} parameter of the parameterized post-Einstein (ppE) framework [110]. Thus the two observables we seek to compute in this Section are the correction to the change in the binary period, \dot{P}_b , and the ppE parameter β_{ppE} . These quantities can be used to project estimated constraints on the theories of interest.

We will consider three example theories. In Sec. VB, we focus on D²GB gravity as an example of shift-symmetric, topological quadratic gravity. We then study two theories which do not satisfy the conditions of the miracle hair loss theorem. In Sec. VC we focus

¹⁰ Technically, this radial coordinate has been transformed from the standard radial coordinate of a non-rotating configuration, following the procedure laid out by Hartle and Thorne [108, 109].

on non-shift-symmetric but topological theories, with TEdGB as an example. Finally in Sec. V D we focus on non-shift-symmetric and non-topological theories, with Kretschmann gravity as an example.

For each theory, we will consider the two cases of binaries without BHs, and binaries with at least one BH. The latter is required for D²GB, which falls under the purview of the theorem, since otherwise dipolar radiation is strongly suppressed. Since both TEdGB and Kretschmann predict that NSs source a non-vanishing scalar charge, binary systems without BHs suffice to stringently constrain these theories (though NS/BH binaries still produce the most stringent projected constraint). The best estimated and projected constraints for each of these theories are summarized in Table I.

A. Dipole Radiation, Binary Pulsars, and Gravitational Waves

Consider a binary system composed of two compact objects (either BHs, NSs, or WDs) with masses m_1 and m_2 and observed, for example, through radio pulsar timing or through future GW detectors. A dynamical scalar field will induce a plethora of corrections to the dynamics of the binary, but, typically, the most important of these is due to the energy flux the field carries away as it evolves. As calculated in e.g. [1, 24, 42], this flux is

$$\dot{E}^{(\theta)} = -\frac{4\pi}{3}\eta^2 \left(\mu_1^{(0)} - \mu_2^{(0)}\right)^2 (v_{12})^8, \quad (73)$$

where $\eta \equiv m_1 m_2 / m^2$ is the symmetric mass ratio, $m \equiv m_1 + m_2$ is the total mass, $\mu_{1,2}^{(0)}$ is the scalar charge of each compact object (we drop higher-spin corrections since NSs spin only slowly as already mentioned in Sec. IV B), and v_{12} is the magnitude of the binary's relative orbital velocity. Observe that $\dot{E}^{(\theta)}$ is a -1 PN order correction¹¹ to the GW energy flux in GR $\dot{E}_{\text{GR}} = -(32/5)\eta^2(v_{12})^{10}$.

For binary pulsars, the most important effect of the scalar energy flux is a modification to the rate of orbital period decay \dot{P}_b , which has already been stringently constrained [22, 23]. The orbital period decay is also modified due to corrections to the binding energy E_b , but these are subdominant in a PN sense. The rate of decay of the orbital period P_b , at leading PN order, can be written as

$$\dot{P}_b = \frac{3}{2} \frac{P_b}{E_b} \left(\dot{E}_{\text{GR}} + \dot{E}^{(\theta)} \right). \quad (74)$$

We consider a binary pulsar whose period derivative is observed to be consistent with the prediction of GR,

with an observational uncertainty given by $\sigma_{\dot{P}_b}$. From this observation, one could infer that the fractional correction due to $\dot{E}^{(\theta)}$ must be smaller than the fractional uncertainty in the measurement and we can estimate

$$\left| \frac{\dot{E}^{(\theta)}}{\dot{E}_{\text{GR}}} \right| \lesssim \left| \frac{\sigma_{\dot{P}_b}}{\dot{P}_b} \right|. \quad (75)$$

Combining Eqs. (73) and (75), one then finds that a binary pulsar observation consistent with GR places a constraint on the scalar charges of roughly

$$\left| \mu_1^{(0)} - \mu_2^{(0)} \right| \lesssim \left| \frac{24}{5\pi} \frac{\sigma_{\dot{P}_b}}{\dot{P}_b} \right|^{1/2} |v_{12}|. \quad (76)$$

Such a bound can be converted into a constraint on $\sqrt{|\alpha_X|}$ once we substitute the explicit forms of the scalar charge on the left-hand side of Eq. (76). Observe that if the binary components have comparable compactnesses (and thus comparable scalar charges), as is the case for NS/NS binary pulsars, then the constraint is weakened. Thus, when a scalar charge is present and a scalar energy flux is sourced, the best systems to constrain such modifications are mixed binaries.

The most important effect of the scalar energy flux in the GWs emitted by binary systems is a modification in the Fourier phase of the waves. This correction can be well-described in the parameterized post-Einsteinian framework of [110]. Performing a stationary phase approximation analysis, the GW phase correction to GR in the Fourier domain is of -1 PN relative order, with magnitude

$$\beta_{\text{ppE}} = -\frac{5\pi}{1792} \left(\mu_1^{(0)} - \mu_2^{(0)} \right)^2 \eta^{2/5}. \quad (77)$$

Consider a future GW measurement that is consistent with GR, meaning that β_{ppE} is consistent with zero with an uncertainty given by $\sigma_{\beta_{\text{ppE}}}$. From such a measurement, we would estimate the projected constraint

$$\left| \mu_1^{(0)} - \mu_2^{(0)} \right| \lesssim \left(\frac{1792}{5\pi} \sigma_{\beta_{\text{ppE}}} \right)^{1/2} \eta^{-1/5}. \quad (78)$$

This bound can be converted into a projected constraint on $\sqrt{|\alpha_X|}$, just as for binary pulsars, by substituting in the explicit forms of the scalar charge on the left-hand side.

When dipole radiation is present in a given theory, binary pulsar observations are better than GW observations to constrain that theory [111]. This is because dipole radiation enters at a pre-Newtonian order relative to GW predictions in GR, which enter through quadrupole radiation at “Newtonian” order. This means that dipole radiation affects observables at $\mathcal{O}(c^2/v_{12}^2)$ relative to the GR expectation. The orbital period of binary pulsars is much larger than that of GW sources of ground-based interferometers, and thus, v_{12} is much smaller, which makes the effect of dipole radiation much larger for binary pulsars.

¹¹ Henceforth, a term proportional to $(m/r_{12})^A$ relative to its leading-order expression will be said to be of APN order, with r_{12} the binary's separation. By the virial theorem, v_{12}^2 is of the same order as m/r_{12} , and thus, a term proportional to $(v_{12})^{2N}$ relative to some other term will be said to be of NPN order.

B. Shift-Symmetric, Non-Derivative, Topological Quadratic Gravity: D²GB Example

Let us take D²GB as an example of quadratic gravity theories with a shift symmetric, non-derivative, topological interaction density. As discussed in Sec. III, NSs will not source scalar charge in this theory, but BHs will. Let us then separate the discussion of constraints into those that come from binaries where at least one of the components is a BH and those where neither component is a BH.

1. Binaries without black holes

Since scalar charge is not sourced in this case, the main modifications to the evolution of the binary is due to higher-order multipole scalar hair and metric deformations induced by modifications to the multipole moments. The latter dominates the former as sketched in App. B and arise through corrections to the moment of inertia and to the quadrupole moment of each individual star. These modifications induce corrections in the rate of decay of the orbital period and to the GW signal, but they are of 1.5 PN order or higher relative to the leading-order term in GR. Therefore, current binary pulsar observations of \dot{P}_b cannot place meaningful constraints on D²GB gravity.

One could, in principle, use other binary pulsar observables to constrain the theory, such as the rate of change of the pericenter $\langle \dot{w} \rangle$. This quantity would be corrected at 0.5PN order relative to GR due to modifications to the star's moment of inertia and at 1PN order due to quadrupole moment deformations. The moment of inertia, however, is very hard to measure [112], and expected errors will be too large to allow for meaningful constraints [106]. Moreover, 1PN corrections to perihelion precession from quadrupole moment deformations would lead to constraints that are outside the regime of validity of the decoupling limit, as is also the case in dynamical Chern-Simons gravity [28].

One could in principle constrain these higher PN effects with GW observations produced in the inspiral of NS binaries. We cannot construct an estimate of these here because the precise form of such corrections is not yet known.

2. Binaries with at least one black hole

Black holes source a scalar charge, so the dynamics of mixed BH/NS systems is strongly corrected. Therefore, the best constraints on quadratic gravity with shift-symmetric, non-derivative, and topological interactions will come from future observations of binary systems where at least one of the binary components is a black

hole.¹² This could be achieved, for example, through future observations of yet unobserved BH/NS pulsar binaries with radio telescopes [113, 114] or through future observations of the GWs emitted by BH/BH or BH/NS binaries [24, 65].

We can estimate the magnitude of the constraints one could achieve on D²GB gravity, given a future BH/NS pulsar observation with the *Five-Hundred-Meter Aperture Spherical Radio Telescope* (FAST) [115] or with the *Square-Kilometer Array* (SKA) [58]. Let us then consider a binary with masses of $m_{\text{BH}} = 10M_{\odot}$ and $m_{\text{NS}} = 1.4M_{\odot}$ in a circular orbit. Substituting the scalar charge of a non-rotating BH, given by Eq. (58) [24, 30–33] to leading order in the coupling constant, and Kepler's law $v_{12} = (2\pi m/P_b)^{1/3}$ in Eq. (76), one obtains the projected bound

$$\left(\sqrt{|\alpha_{\text{GB}}|}\right)_{\text{BHNS}}^{\text{Bin.Pul.}} \lesssim 0.12 \text{ km} \left(\frac{m_{\text{BH}}}{10M_{\odot}}\right) \left(\frac{m}{11.4M_{\odot}}\right)^{1/6} \times \left(\frac{\sigma_{\dot{P}_b}/\dot{P}_b}{10^{-2}}\right)^{1/4} \left(\frac{P_b}{3 \text{ days}}\right)^{-1/6}. \quad (79)$$

The contours of Fig. 4 show estimates of the upper bound on $\sqrt{|\alpha_{\text{GB}}|}$ [km] from Eq. (79), as a function of $|\sigma_{\dot{P}_b}/\dot{P}_b|$ and P_b . Reference [114] estimated the accuracy to which FAST and SKA, as well as a 100-meter radio dish for reference, would be able to measure the orbital period decay as a function of the orbital period [114]. Figure 4 shows these estimates with solid, dashed or dotted curves, assuming a 3 or a 5 year observation. Given an observation of the orbital decay rate consistent with GR and with period $P_{b,\text{obs}}$, one obtains a point in this figure that must lie on one of the observation curves (either the 100 meter, FAST or SKA curves), which would then place an estimated constraint on $\sqrt{|\alpha_{\text{GB}}|}$ shown by the contours.

Let us now estimate the magnitude of the constraints one could achieve on D²GB gravity with a future GW observation with aLIGO of the late inspiral of a compact binary. Cornish et al. [111] found that given an aLIGO GW observation with signal-to-noise ratio (SNR) of 20, one could assert that β_{ppE} is zero up to an uncertainty of roughly $\sigma_{\beta_{\text{ppE}}} = 5 \times 10^{-4}$. Using this projected uncertainty and Eq. (78), we find the projected bound

$$\left(\sqrt{|\alpha_{\text{GB}}|}\right)_{\text{BHNS}}^{\text{GW}} \lesssim 3.0 \text{ km} \left(\frac{\sigma_{\beta_{\text{ppE}}}}{5 \times 10^{-4}}\right)^{1/4} \left(\frac{m_{\text{BH}}}{5M_{\odot}}\right) \left(\frac{0.171}{\eta}\right)^{1/10} \quad (80)$$

¹² In dynamical Chern-Simons gravity, BHs do not possess a scalar charge, but it is still true that the best constraints come from BH binaries. This is because the leading correction to the binary evolution in this theory enters at 2PN order and is proportional to spin squared [24, 27, 28]. Since black holes spin much faster than NSs in general, BH binaries will place constraints that are stronger than NS binaries [27, 28].

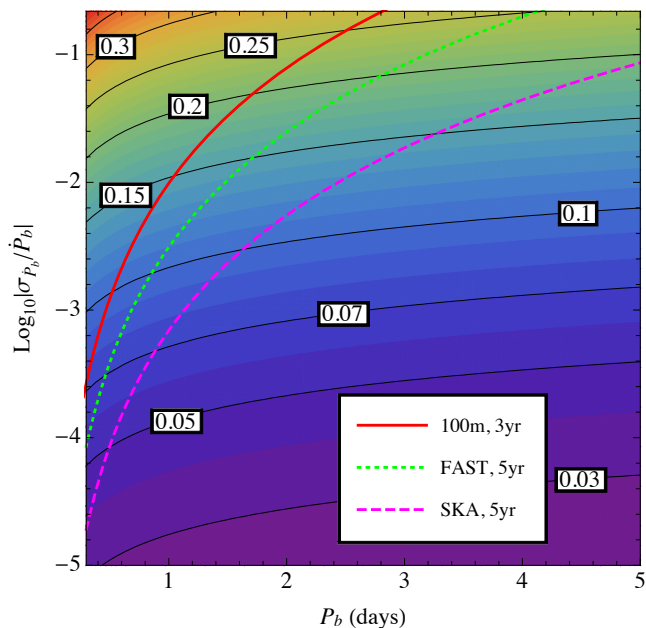


FIG. 4. (Color online) Upper bound on the theory coupling parameter $|\alpha_{\text{GB}}|^{1/2}$ in D^2GB gravity in units of kilometers as a function of orbital period and the measurement accuracies of the orbital period decay rate of a BH/NS binary pulsar [Eq. (79)]. We also show the projected accuracy of the measurement of the orbital period decay rate with a 100 meter antenna (red solid curve), FAST (green dotted curve) and SKA (magenta dashed curve), as a function of orbital period. Given observations of the orbital period decay rate with this predicted accuracy, one would be able to constrain D^2GB gravity one order of magnitude more stringently than the current estimated bound.

for a $(1.4, 5)M_{\odot}$ NS/BH binary, and

$$\left(\sqrt{|\alpha_{\text{GB}}|}\right)_{\text{BHBH}}^{\text{GW}} \lesssim 3.4 \text{ km} \left(\frac{\sigma_{\beta_{\text{PDE}}}}{5 \times 10^{-4}}\right)^{1/4} \left(\frac{m}{15M_{\odot}}\right) \left(\frac{0.33}{\delta m/m}\right)^{1/2} \left(\frac{\eta}{0.22}\right)^{9/10} \quad (81)$$

for a $(10, 5)M_{\odot}$ BH/BH binary, where $\delta m \equiv m_1 - m_2$. Eq. (81) is in agreement with [24], where the constraint was first calculated.

How do these future constraints compare to current constraints? Recall that the observation of LMXBs has implied the constraint $\sqrt{|\alpha_{\text{GB}}|} < 1.9 \text{ km}$ [65]. We then see that pulsar observations would be able to improve this constraint by 1 order of magnitude, while GW observations would lead to comparable constraints. One concludes that binary pulsars will be better at constraining dipole radiation than GW observations, provided a BH/pulsar binary is observed. These results are in agreement with those found in [111].

C. Non-Shift-Symmetric, Topological Quadratic Gravity: TEdGB Example

Let us take TEdGB as an example of quadratic gravity theories with a non-shift-symmetric, non-derivative, topological interaction density. This time, NSs do source a scalar charge, and thus, BHs are not needed to activate scalar energy flux correction. We then expect that binary pulsar observations of NS/WD and NS/NS systems will lead to strong estimated constraints. As before, we separate the discussion into observations that involve binaries with at least one BH and those without BHs.

1. Binaries without black holes

Let us first concentrate on radio pulsar observations. The best constraints on TEdGB using binaries without BHs will come from mixed NS/WD observations, as these will have the most dissimilar compactnesses, and thus, the difference in the scalar charges will not be inherently small. Using the leading-order term of Eq. (69) with a Tolman VII model in a $C \ll 1$ expansion, and choosing $\gamma = 1$ and $\vartheta_{\infty} = 0$ to be consistent with [106], one finds the estimated constraint

$$\left(\sqrt{|\alpha_{\text{TEdGB}}|}\right)_{\text{NSWD}}^{\text{Bin.Pul.}} \lesssim 1.4 \text{ km} \left(\frac{m_{\text{NS}}}{1.46M_{\odot}}\right)^{-3/4} \left(\frac{R_{\text{NS}}}{12\text{km}}\right)^{7/4} \times \left(\frac{|v_{12}/c|}{1.2 \times 10^{-3}}\right)^{1/4} \left(\frac{\sigma_{\dot{P}_b}/\dot{P}_b}{6.1 \times 10^{-2}}\right)^{1/8}. \quad (82)$$

The values of the NS mass, the orbital velocity and the observational error that we chose to normalize the above constraint are those of J1738+0333 [22].

The estimate found above clearly depends on the NS radius R_{NS} , because this quantity unavoidably enters the NS charge. Figure 5 shows this dependence for a Tolman VII model and an $n = 0$ polytropic model using the mass, orbital velocity and measurement accuracy of J1738+0333 [22]. Observe that the estimated constraints are always between 1 and 2km for the Tolman VII model, which recall is a more realistic equation of state than an $n = 0$ polytrope. Observe also that the bounds on TEdGB gravity are comparable to the best current bounds that uses the existence of BH solutions [50, 51]. We have also studied the bound one could place on α_{TEdGB} from observations of the WD/NS pulsar binary J0348+0432 [116] and found it to be slightly weaker.

A similar constraint can be derived from the observation of the double NS pulsar binary J0737-3039 [21]. Following the same procedure as that described above, but this time keeping both scalar charges, we find the

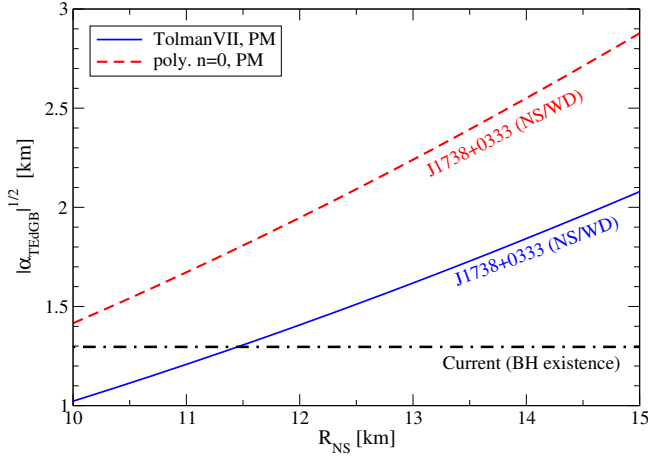


FIG. 5. (Color online) Upper bound on $\sqrt{|\alpha_{\text{TEdGB}}|}$ from observations of the orbital decay rate of J1738+0333 [22] as a function of the NS radius with $\gamma = 1$ and $\vartheta_\infty = 0$. For this constraint, we use the analytic post-Minkowskian calculation of the scalar charge with a Tolman VII and an $n = 0$ polytropic equation of state (Eqs. (68) and (69)). For comparison, we also include the most stringent current constraint based on BH existence considerations [50, 51].

estimated constraint

$$\begin{aligned} \left(\sqrt{|\alpha_{\text{TEdGB}}|}\right)_{\text{NSNS}}^{\text{Bin.Pul.}} &\lesssim 1.7 \text{ km} \left(\frac{R_1}{11.5 \text{ km}}\right)^{7/4} \left(\frac{R_2}{12 \text{ km}}\right)^{7/4} \\ &\quad \left(\frac{|v_{12}/c|}{2.08 \times 10^{-3}}\right)^{1/4} \left(\frac{\sigma_{\dot{p}_b}/\dot{P}_b}{1.7 \times 10^{-2}}\right)^{1/8} \\ &\quad \left[\left(\frac{m_1}{1.337 M_\odot}\right)^3 \left(\frac{R_2}{12 \text{ km}}\right)^7 \right. \\ &\quad \left. - \left(\frac{m_2}{1.250 M_\odot}\right)^3 \left(\frac{R_1}{11.5 \text{ km}}\right)^7 \right]^{-1/4}, \end{aligned} \quad (83)$$

where we have assumed that $m_1 > m_2$, and thus, $R_2 \geq R_1$. Observe that this constraint is comparable but slightly weaker than those obtained with J1738+0333. This is because in the double NS binary pulsar case there is a natural suppression in the amount of scalar energy flux emitted due to the comparable masses of the system, i.e. when $m_1 \sim m_2$, then $\mu_1 \approx \mu_2$ and thus $E^{(\vartheta)}$ is suppressed. Observe also that this constraint depends on the radii of both NSs. Varying the radii of Eq. (83), we find that the estimated constraint varies between roughly 1.5 and 3.5 km.

Let us now estimate the magnitude of the constraints one could achieve on TEdGB gravity with a future GW observation. As in Sec. VB, we assume an aLIGO observation of the late inspiral of a NS/NS binary with an SNR of 20. Setting $\gamma = 1$ and $\vartheta_\infty = 0$, we find the

projected constraint

$$\begin{aligned} \left(\sqrt{|\alpha_{\text{TEdGB}}|}\right)_{\text{NSNS}}^{\text{GW}} &\lesssim 7.9 \text{ km} \left(\frac{\sigma_{\text{ppE}}}{5 \times 10^{-4}}\right)^{1/8} \left(\frac{R_1}{11.5 \text{ km}}\right)^{7/4} \\ &\quad \left(\frac{R_2}{12 \text{ km}}\right)^{7/4} \left(\frac{0.249}{\eta}\right)^{1/20} \\ &\quad \left[\left(\frac{m_1}{1.6 M_\odot}\right)^3 \left(\frac{R_2}{12 \text{ km}}\right)^7 \right. \\ &\quad \left. - \left(\frac{m_2}{1.4 M_\odot}\right)^3 \left(\frac{R_1}{11.5 \text{ km}}\right)^7 \right]^{-1/4}. \end{aligned} \quad (84)$$

As before, these projected constraints also depend on the radii of both NSs. Varying these parameters, we find the constraint is always between 6 and 14 km. Once more, we see that the projected constraints we could place with GWs are weaker than the estimated constraints with J1738+0333. This is because in TEdGB the scalar charge does not vanish, thus exciting dipole radiation which enters at a pre-Newtonian order and could be better constrained by binary pulsar observations, as discussed in Sec. VA.

2. Binaries with at least one black hole

Let us first discuss future binary pulsar observations where one component of the binary is a BH. The correction to the scalar energy flux is then dominated by the scalar charge of the BH, which we model through Eq. (58). This scaling from the D²GB limit agrees with what is found in analytic calculations in TEdGB [50]. Given this, the projected constraint with a future BH-pulsar binary observation is the same as that in Eq. (79) and Fig. 4. Such projected bounds are roughly an order of magnitude stronger than the estimated constraints that use binary systems without BHs.

Let us now consider projected constraints with GW observations. As in Sec. VB, let us assume an aLIGO observation with an SNR of 20 of the late inspiral of a compact binary. Setting $\gamma = 1$ and $\vartheta_\infty = 0$, we find the same projected constraints as those in Eq. (80) for a NS/BH inspiral and Eq. (81) for a BH/BH binary inspiral observation. In both cases, this is because both constraints use the same BH scalar charge as in D²GB. We see again that both constraints improve by roughly an order of magnitude when including BHs relative to those of Sec. VC1. But again, these GW constraints would be weaker than binary pulsar constraints, if the latter observed a BH/pulsar system.

How do these future constraints compare to current constraints? Recall that current constraints on TEdGB gravity come from BH existence considerations, which require that $\sqrt{|\alpha_{\text{TEdGB}}|} < 1.4 \text{ km}$ [50, 51]. We then see that projected constraints with BH/pulsar observations will improve this bound by one order of magnitude, while projected GW constraints will be comparable or slightly weaker than current constraints.

D. Non-Shift-Symmetric, Non-Topological Quadratic Gravity: Kretschmann Example

Let us take Kretschmann gravity as an example of quadratic gravity theories with a non-shift-symmetric, non-derivative, non-topological interaction density. As in the TEdGB case, NSs do source a scalar charge, and once more, BHs are not needed to activate corrections to the dynamics due to the scalar energy flux. We therefore expect radio pulsar observations of NS/WD and NS/NS binaries to lead to strong estimated bounds. We again separate the discussion into observations that include binaries with at least one BH and those without BHs.

1. Binaries without black holes

Let us first focus on binary pulsar observations. As in the previous cases, the dominant correction to the energy flux is given by Eq. (73). In order to obtain estimated constraints on Kretschmann gravity, we use the post-Minkowskian result for $\mu_{\kappa}^{(0)}$ with the Tolman VII model given in Eq. (67). For a WD/NS binary pulsar, Eq. (76) leads to the estimated constraint

$$\left(\sqrt{|\alpha_{\kappa}|}\right)_{\text{NSWD}}^{\text{Bin.Pul.}} \lesssim 0.076 \text{ km} \left(\frac{m_{\text{NS}}}{1.46M_{\odot}}\right)^{-1/2} \left(\frac{R_{\text{NS}}}{12\text{km}}\right)^{3/2} \left(\frac{|v_{12}/c|}{1.2 \times 10^{-3}}\right)^{1/2} \left(\frac{\sigma_{\dot{P}_b}/\dot{P}_b}{6.1 \times 10^{-2}}\right)^{1/4}. \quad (85)$$

Observe that this is a rather strong estimated constraint, when compared to those found in D²GB gravity and TEdGB gravity.

As in the TEdGB gravity case, the estimated binary pulsar constraints depend on the NS radius. Figure 6 shows the upper bound on $\sqrt{|\alpha_{\kappa}|}$ from the \dot{P}_b measurement of J1738+0333 [22] and J0348+0432 [116] as a function of NS radius for a set of tabulated equations of state. The scalar charge of a non-rotating NS with such equations of state in Kretschmann gravity is calculated numerically as explained in Sec. IV A. The observation of J1738+0333 places a stronger constraint than the observation of J0348+0432 because \dot{P}_b for the former has been measured more accurately. For comparison, we also present constraints using the leading-order, post-Minkowskian expression for the scalar charge with an $n = 0$ polytropic model and the Tolman VII model. Observe that the constraints using realistic equations of state lie very close to those obtained using the Tolman VII model. We also show the constraint on D²GB gravity using observations of A0620-00 [65]. Although one cannot directly compare estimated constraints on two different theories and in different types of systems, this difference suggests that the absence of NS scalar charge in D²GB reduces our constraining power by an order of magnitude in that theory. Meanwhile, the projected constraint on Kretschmann gravity estimated here is comparable to the projected constraint on D²GB gravity

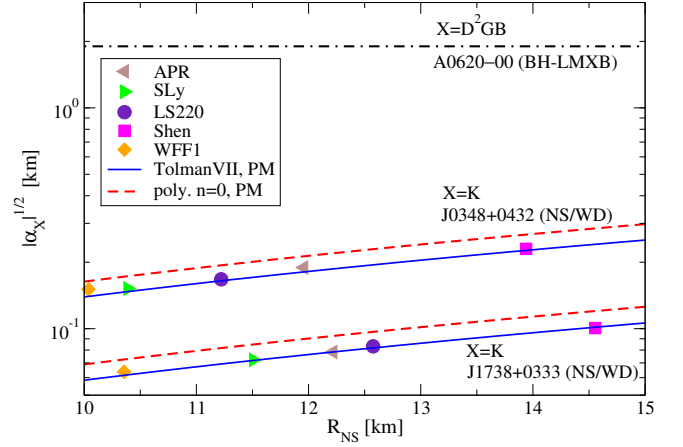


FIG. 6. (Color online) Upper bound on $\sqrt{|\alpha_{\kappa}|}$ in Kretschmann gravity from observations of the orbital period decay of J1738+0333 [22] and J0348+0432 [116] with various equations of state as a function of NS radius. Solid and dashed curves represent the bound using a Tolman VII model and an $n = 0$ polytropic model respectively, and to leading-order in the post-Minkowskian approximation. For reference, we also present the bound on D²GB gravity from observations of A0620-00 [65].

estimated for a BH/pulsar binary presented in Sec. V B 2 and summarized in Fig. 4.

We can repeat the above calculation for a binary pulsar composed of two NSs. Doing so, we find the estimated constraint

$$\left(\sqrt{|\alpha_{\kappa}|}\right)_{\text{NSNS}}^{\text{Bin.Pul.}} \lesssim 0.19 \text{ km} \left(\frac{R_1}{11.5\text{km}}\right)^{3/2} \left(\frac{R_2}{12\text{km}}\right)^{3/2} \left(\frac{|v_{12}/c|}{2.08 \times 10^{-3}}\right)^{1/2} \left(\frac{\sigma_{\dot{P}_b}/\dot{P}_b}{2.87 \times 10^{-2}}\right)^{1/4} \left[\left(\frac{m_1}{1.337M_{\odot}}\right) \left(\frac{R_2}{12\text{km}}\right)^3 - \left(\frac{m_2}{1.250M_{\odot}}\right) \left(\frac{R_1}{11.5\text{km}}\right)^3\right]^{-1/2}. \quad (86)$$

Observe that this is weaker than that found for WD/NS pulsar binary systems [Eq. (85)], in spite of the latter typically being less relativistic and having less accurate \dot{P}_b measurement. Observe also that this estimated constraint depends on both NS radii; varying both of these, we find that the estimated constraint ranges between 0.15 and 0.45 km, and of course it becomes stronger as the uncertainty in the measurement of \dot{P}_b decreases.

Let us now discuss projected GW constraints on Kretschmann gravity with signals emitted in the inspiral of NS binaries. Let us once more assume an aLIGO detection with SNR 20. Then, using Eq. (78) and the post-Minkowskian result for $\mu_{\kappa}^{(0)}$ with the Tolman VII

model given in Eq. (67), we find the estimated constraint

$$\begin{aligned} \left(\sqrt{|\alpha_{\kappa}|}\right)_{\text{NSNS}}^{\text{GW}} &\lesssim 4.1 \text{ km} \left(\frac{\sigma_{\beta_{\text{ppE}}}}{5 \times 10^{-4}}\right)^{1/4} \left(\frac{R_1}{11.5 \text{ km}}\right)^{3/2} \\ &\quad \left(\frac{R_2}{12 \text{ km}}\right)^{3/2} \left(\frac{0.249}{\eta}\right)^{1/10} \\ &\quad \left[\left(\frac{m_1}{1.6 M_{\odot}}\right) \left(\frac{R_2}{12 \text{ km}}\right)^3 \right. \\ &\quad \left. - \left(\frac{m_2}{1.4 M_{\odot}}\right) \left(\frac{R_1}{11.5 \text{ km}}\right)^3\right]^{-1/2}. \end{aligned} \quad (87)$$

As expected, this constraint depends on the radii of both NSs; varying these quantities, we find the estimated constraint ranges between 3 and 9 km. Observe that this is roughly one order of magnitude weaker than binary pulsar constraints.

2. Binaries with at least one black hole

Future radio observations of BH/NS pulsar binaries could lead to complementary constraints. Since vacuum solutions in D²GB gravity are also solutions in Kretschmann gravity with the identification $\alpha_{\text{GB}} = \alpha_{\kappa}$, we can use some of the results from Sec. VB2. Let us then again use Eq. (76), with the NS scalar charge modeled through Eq. (67) and the BH scalar charge through Eq. (58). We then find the projected constraint

$$\begin{aligned} \left(\sqrt{|\alpha_{\kappa}|}\right)_{\text{BHNS}}^{\text{Bin.Pul.}} &\lesssim 0.049 \text{ km} \left(\frac{R_{\text{NS}}}{12 \text{ km}}\right)^{3/2} \left(\frac{m_{\text{BH}}}{10 M_{\odot}}\right) \left(\frac{|v_{12}/c|}{10^{-3}}\right)^{1/2} \\ &\quad \left(\frac{\sigma_{\dot{P}_b}/\dot{P}_b}{10^{-2}}\right)^{1/4} \left[7 \left(\frac{R_{\text{NS}}}{12 \text{ km}}\right)^3 \right. \\ &\quad \left. + 180 \left(\frac{m_{\text{NS}}}{1.4 M_{\odot}}\right) \left(\frac{m_{\text{BH}}}{10 M_{\odot}}\right)^2\right]^{-1/2}. \end{aligned} \quad (88)$$

This projected constraint varies between 0.036 and 0.074 km as one varies the NS radius. Notice that such a constraint is 2–3 times stronger than that on D²GB gravity for the same system observed [compare to Eq. (79)]. This is because the NS scalar charge in Kretschmann gravity dominates the BH scalar charge, which leads to enhanced scalar dipole radiation compared to the D²GB case, where the stellar scalar charge vanishes. The projected constraints in Fig. 4 are also valid in Kretschmann gravity as an order of magnitude estimate, with the contours representing an upper bound on $\sqrt{|\alpha_{\kappa}|}$.

Let us now discuss GW observations, assuming once more an aLIGO detection with SNR 20. Using Eq. (78), with the neutron scalar charge modeled through Eq. (67) and the BH charge through Eq. (58), we find the pro-

jected constraint

$$\begin{aligned} \left(\sqrt{|\alpha_{\kappa}|}\right)_{\text{BHNS}}^{\text{GW}} &\lesssim 2.5 \text{ km} \left(\frac{m_{\text{BH}}}{10 M_{\odot}}\right) \left(\frac{R_{\text{NS}}}{11.5 \text{ km}}\right)^{3/2} \\ &\quad \left(\frac{0.1}{\eta}\right)^{1/10} \left(\frac{\sigma_{\beta_{\text{ppE}}}}{5 \times 10^{-4}}\right)^{1/4} \left[7 \left(\frac{R_{\text{NS}}}{12 \text{ km}}\right)^3 \right. \\ &\quad \left. + 180 \left(\frac{m_{\text{NS}}}{1.4 M_{\odot}}\right) \left(\frac{m_{\text{BH}}}{10 M_{\odot}}\right)^2\right]^{-1/2} \end{aligned} \quad (89)$$

for a BH/NS inspiral. Varying the radius of the NS, we find that the projected constraint varies between 2.0 and 4.1 km. Similarly, for a BH/BH inspiral, we find projected constraints that are identical to Eq. (81), since both use the same BH scalar charge. As expected, the projected constraints are roughly two orders of magnitude weaker than those that could be placed with BH/pulsar binaries.

VI. CONCLUSIONS AND FUTURE DIRECTIONS

Many people may believe that gravity theories with a long-ranged scalar field are tightly constrained by binary pulsar observations. This is because many theories with a long-ranged scalar field have been proposed, where NSs source a spherically symmetric, $1/r$ scalar hair (a scalar charge). An accelerating charge produces dipole radiation, but the effects of dipole radiation have been strongly constrained by binary pulsar observations.

In this paper we have addressed and tried to dispel this lore. We first classified the relevant theories in terms of whether each theory has (i) shift symmetry, (ii) a coupling to a topological density, and (iii) derivative or non-derivative interactions between the scalar field and the metric. We conjecture that theories with a shift-symmetric scalar field sourced by a linear (non-derivative) coupling to a topological density do not activate a scalar charge in NSs.

We proved this theorem specifically for D²GB gravity, which is an example of this class. Our rigorous proof is based on the generalized Gauss-Bonnet-Chern theorem, and improves upon the “physicist’s” proof given in [24], which was only valid for static, spherically symmetric stars. We confirmed the absence of the NS scalar charge in this theory by explicitly calculating the scalar field around a slowly-rotating star to quadratic order in spin, both analytically within the weak-field expansion and numerically in the strong-field case.

Therefore, in order to place meaningful constraints on D²GB gravity, one needs to use observations of compact binaries that contain at least one BH. The current estimated constraint on the theory using a BH-LMXB was derived in [49]. We here derived projected constraints from radio observations of BH/pulsar binaries and GW observations of NS/BH and BH/BH binaries. We found that radio observations could place constraints that are

one order of magnitude stronger than the current bound, while GW constraints would be slightly weaker than the current one.

We also derived estimated and projected constraints on (i) TEdGB and (ii) Kretschmann gravity as examples of (i) non-shift-symmetric but topological, and (ii) non-shift-symmetric and non-topological theories respectively. In both cases, we found that ordinary stars acquire a scalar charge, and hence, current binary pulsar observations are sufficient in constraining these theories. We found that such binary pulsar constraints are comparable to the current bound from the existence of BH solutions in TEdGB, while they are stronger than the current bound from a BH-LMXB by roughly one order of magnitude in Kretschmann gravity. We also found that future BH/pulsar observations could improve current binary pulsar constraints by roughly one order of magnitude.

Let us comment on the relation between the scalar charge, defined in this paper as the spherically symmetric, $1/r$ coefficient of the scalar field in a far-field expansion, and the derivative of the ADM mass with respect to the scalar field at spatial infinity, as is routinely done in scalar-tensor theories. In such theories, one can calculate the variation of the ADM mass from the variation of the Lagrangian with respect to the metric and the scalar and matter fields [117]. Then, the authors in [117] prove that the $1/r$ coefficient in the scalar field is equivalent to the derivative of the ADM mass with respect to the scalar field at infinity. In fact, this approach has already been applied to Einstein-Æther and khronometric theories in [118]. If one applies this approach to D^2 GB gravity, one finds that the variation of the stellar ADM mass with respect to the scalar field vanishes [29], in agreement with the vanishing scalar charge found in this paper.

A. Future work

One natural extension of this work would consider the Pontryagin density, rather than the Gauss-Bonnet density, as the topological invariant to which the scalar couples. Whereas the integral of the Gauss-Bonnet density is related to the manifold's Euler characteristic, the integral of the Pontryagin density is related to the first Pontryagin number. The proof should be similar in spirit to the one presented here. However, it requires understanding a different theorem on a pseudo-Riemannian manifold with boundary.

A second natural and very straightforward extension is to consider BH spacetimes. We may already outline what happens to our proof in the BH case. Firstly, the integration region would consist of a spherical annulus crossed with a compactified time interval. The outer boundary is treated the same as here, but the inner boundary is a null surface—the Killing horizon of the BH. The Euler characteristic is unchanged. However,

both sides of the equality relating the boundary integrals [Eq. (41)] need to include both the inner and outer boundaries. The inner boundary will in fact contribute in this calculation. We will find that the scalar charge is proportional to a horizon integral, and from scaling arguments we see that we will recover the known scaling $\mu \sim 1/m_{\text{BH}}$ [24, 30–33]. This approach can potentially connect to the thermodynamics of Gauss-Bonnet BHs.

Yet a third natural extension is to derive a proposed bound on dynamical Chern-Simons gravity with BH/NS pulsar observations. Corrections to some of the post-Keplerian parameters in this theory have been derived in [28], which are absent if bodies are non-rotating. One can extend the analysis in [114] by including such corrections to the binary evolution and study how well one can constrain the theory with a rotating BH/pulsar observations. If the observation is accurate enough, one should be able to derive an upper bound on $\sqrt{|\alpha_{\text{CS}}|}$ that is comparable to the size of a BH. If this is the case, one would obtain a constraint comparable to that projected using future GW observations derived in [27], which is six orders of magnitude stronger than the current bound.

Finally, a fourth extension is the same problem but in a cosmological setting. In this case, the spacetime is no longer asymptotically flat. Therefore, the calculations presented in this paper do not apply, and NSs may acquire a scalar charge in D^2 GB gravity. However, it is not clear how to define multiple moments of the metric and scalar fields in a cosmological setting.

ACKNOWLEDGMENTS

The authors thank Enrico Barausse, Mike Boyle, Gilles Esposito-Farèse, Paulo Freire, Takahiro Tanaka, and Norbert Wex for useful discussions and comments. We also thank Paolo Pani for providing us numerical data on the scalar charge in TEdGB gravity to compare against. L.C.S. and N.Y. would like to thank the Max Planck Institute for Radioastronomy for their hospitality, while this work was started. K.Y. acknowledges support from JSPS Postdoctoral Fellowships for Research Abroad and the NSF grant PHY-1305682. L.C.S. acknowledges that support for this work was provided by NASA through Einstein Postdoctoral Fellowship Award Number PF2-130101 issued by the Chandra X-ray Observatory Center, which is operated by the Smithsonian Astrophysical Observatory for and on behalf of the NASA under contract NAS8-03060, and further acknowledges support from the NSF grant PHY-1404569. N.Y. acknowledges support from NSF CAREER Grant PHY-1250636. Some calculations used the computer algebra system MAPLE, in combination with the GRTESENSORII package [119].

Appendix A: Details of Calculating Neutron Star Scalar Charge in Quadratic Gravity

In this appendix, we describe details of how one calculate the scalar monopole charge in quadratic gravity, both analytically and numerically. We focus on the $l = 0$ mode since the scalar charge enters through this mode. We concentrate on the even-parity sector of the theory, namely, setting $f_4 = 0$ in the action in Eq. (15) (or $\alpha_4 = 0$ in Eq. (56)).

1. Field Equations and Exterior Solutions

We first present the field equations and exterior solutions for NSs in quadratic gravity. We assume matter to be described by a perfect fluid and use the same metric ansatz as that proposed by Hartle and Thorne [108, 109].

$$\begin{aligned} \vartheta_{\text{ext}}^{(0,1/2)} &= -\frac{2}{M_* r} \left[\alpha_3 \gamma e^{-\gamma \vartheta_\infty} \left(1 + \frac{M_*}{r} + \frac{4}{3} \frac{M_*^2}{r^2} \right) + \frac{1}{4} \left(\mu^{(0,1/2)} M_*^2 + 2\alpha_3 \gamma e^{-\gamma \vartheta_\infty} \right) \frac{r}{M_*} \ln \left(1 - \frac{2M_*}{r} \right) \right], \quad (\text{A3}) \\ \vartheta_{\text{ext}}^{(0,1)} &= \frac{11}{6 M_*^4 r} \left\{ \left[\frac{147}{110} \alpha_3^2 \gamma^3 e^{-2\gamma \vartheta_\infty} \left(1 - \frac{40}{49} \frac{M_*}{r} - \frac{40}{49} \frac{M_*^2}{r^2} - \frac{160}{147} \frac{M_*^3}{r^3} \right) \right. \right. \\ &\quad \left. \left. + \mu^{(0,1/2)} \alpha_3 \gamma^2 e^{-\gamma \vartheta_\infty} M_*^2 \left(1 - \frac{6}{11} \frac{M_*}{r} - \frac{6}{11} \frac{M_*^2}{r^2} - \frac{8}{11} \frac{M_*^3}{r^3} \right) - \frac{3}{11} \mu^{(0,1)} M_*^4 \right] r \ln \left(1 - \frac{2M_*}{r} \right) \right. \\ &\quad \left. + 2\alpha_3 \gamma^2 M_* \left[\frac{147}{110} \alpha_3 \gamma e^{-2\gamma \vartheta_\infty} \left(1 + \frac{9}{49} \frac{M_*}{r} - \frac{44}{147} \frac{M_*^2}{r^2} - \frac{146}{147} \frac{M_*^3}{r^3} - \frac{64}{105} \frac{M_*^4}{r^4} - \frac{160}{441} \frac{M_*^4}{r^4} \right) \right. \right. \\ &\quad \left. \left. + \mu^{(0,1/2)} M_*^2 e^{-\gamma \vartheta_\infty} \left(1 - \frac{5}{11} \frac{M_*}{r} - \frac{8}{33} \frac{M_*^2}{r^2} \right) \right] \right\}, \quad (\text{A4}) \end{aligned}$$

where we decomposed $\mu^{(0)}$ within the small coupling approximation in a similar manner to Eq. (A2) as

$$\mu^{(0)} = \mu^{(0,1/2)} + \mu^{(0,1)} + \mathcal{O}(\zeta^{3/2}). \quad (\text{A5})$$

We have also used the exterior solutions for the metric in GR, which is justified since the quadratic gravity correction to the metric only affects the scalar field exterior solution at $\mathcal{O}(\zeta^{3/2})$, even when ϑ_∞ does not vanish. This is because the non-shift-symmetric contribution to the metric field equations vanish in the exterior region, and hence, $\mathcal{O}(\zeta^{1/2})$ contribution sourced by ϑ_∞ is absent in the metric exterior solution. Notice that $\mu^{(0,1/2)}$ and $\mu^{(0,1)}$ are the only integration constants, which by construction coincide with the scalar charge, because we have removed the other constants through a redefinition of the constant ϑ_∞ in Eq. (27).

a. Non-rotating Neutron Stars

Let us first consider non-rotating NSs with the coupling function in the action given by Eq. (62). The field equation is given by Eq. (60) with $S^{(0)}$ given by

$$S^{(0)} = \frac{8}{r^5(r-2M)} \gamma e^{-\gamma \vartheta^{(0)}} \left\{ 2\alpha_3 M(3M - 8\pi \rho r^3) + \pi^2 r^6 [49\alpha_{\text{GB},1} p^2 + 8\alpha_{\text{GB},2} \rho^2 - 16(3\alpha_1 - \alpha_3)p\rho] \right\}. \quad (\text{A1})$$

We decompose the scalar field $\vartheta^{(0)}$ in a manner similar to Eq. (27):

$$\vartheta^{(0)}(r) = \vartheta_\infty + \vartheta^{(0,1/2)}(r) + \vartheta^{(0,1)}(r) + \mathcal{O}(\zeta^{3/2}), \quad (\text{A2})$$

where $\vartheta^{(0,A)} = \mathcal{O}(\zeta^A)$. Decomposing the field equation within the small coupling approximation using Eq. (A2) and setting $p = 0 = \rho$ and $M = M_*$, one can solve for the exterior solutions and find

b. Slowly-rotating Neutron Stars

Next, we derive the scalar field equations and exterior solutions for slowly-rotating NSs. We assume the scalar coupling function is given by

$$g(\vartheta) = \vartheta, \quad (\text{A6})$$

which is a subclass of the non-linear function of Eq. (62) used in Sec. A1 a by taking the limit $\gamma \rightarrow 0$ while replacing α_i to $-\alpha_i/\gamma$ and keeping this new α_i constant. The purpose of calculating the scalar charge with the linear coupling function is to demonstrate explicitly that the charge vanishes in the D²GB limit. Following Eq. (A2), we decompose $\vartheta_l^{(2)}$ as

$$\vartheta_l^{(2)}(r) = \vartheta_l^{(2,1/2)}(r) + \vartheta_l^{(2,1)}(r) + \mathcal{O}(\zeta^{3/2}), \quad (l = 0, 2), \quad (\text{A7})$$

where $\vartheta_l^{(2,A)} = \mathcal{O}[(M_*\Omega)^2, \zeta^A]$ and $\vartheta_l^{(2)}(\infty)$ can be set to zero without loss of generality. For a linear scalar

field coupling function, the $\mathcal{O}(\zeta)$ contribution vanishes ($\vartheta_0^{(2,1)} = 0$) in the exterior region, and hence, one only needs to calculate $\vartheta_0^{(2,1/2)}$. The scalar field equation and the exterior solutions for non-rotating NSs with the linear coupling function can easily be derived from the results

in Sec. A 1 a with the mapping explained above as

$$S^{(0)} = -\frac{8}{r^5(r-2M)} \left\{ 2\alpha_3 M(3M - 8\pi\rho r^3) + \pi^2 r^6 [49\alpha_{\text{GB},1} p^2 + 8\alpha_{\text{GB},2} \rho^2 - 16(3\alpha_1 - \alpha_3) p \rho] \right\}, \quad (\text{A8})$$

$$\vartheta_{\text{ext}}^{(0,1/2)} = \frac{2}{M_* r} \left[\alpha_3 \left(1 + \frac{M_*}{r} + \frac{4}{3} \frac{M_*^2}{r^2} \right) - \frac{1}{4} \left(\mu^{(0,1/2)} M_*^2 - 2\alpha_3 \right) \frac{r}{M_*} \ln \left(1 - \frac{2M_*}{r} \right) \right]. \quad (\text{A9})$$

Regarding the scalar field equation at second order in spin, $\vartheta_0^{(2)}$ obeys the same equation as Eq. (60), except $S^{(0)}$ needs to be replaced by $S^{(2)}$, which is given by

$$\begin{aligned} S^{(2)} = & \frac{1}{6r^6(r-2M)^3} \left\{ 1024r^5(r-2M)e^{-\nu} \left[-\frac{(r-2M)\omega_1'^2}{32} \left[-\frac{1}{32}r^4(r-2M)\vartheta^{(0)'} - 2\alpha_3 M^2 \right. \right. \right. \\ & + \alpha_3 \left(\pi\rho r^2 + \pi p r^2 + \frac{7}{2} \right) rM + r^2 \left(\pi^2(\alpha_{\text{GB},1} - \alpha_{\text{GB},2})r^4\rho^2 - \pi^2(\alpha_{\text{GB},1} + \alpha_{\text{GB},2})r^4 p \rho - 2\pi^2\alpha_{\text{GB},1}r^4 p^2 - \frac{5}{4}\alpha_3 \right) \left. \right. \\ & \left. - \frac{\pi}{4}(\rho + p)r^2(r-2M)\omega_1\omega_1' \left\{ -\alpha_3 M + r \left[\pi(\alpha_{\text{GB},1} - \alpha_{\text{GB},2})r^2\rho - 2\pi\alpha_{\text{GB},1}r^2 p + \alpha_3 \right] \right\} \right. \\ & + \pi(\rho + p)r\omega_1^2 \left\{ \frac{1}{64}r^4(r-2M)\vartheta^{(0)'} - \frac{3}{4}\alpha_3 M^2 + \frac{3}{4}r \left[(\alpha_{\text{GB},1} - \alpha_{\text{GB},2})\pi r^2\rho - 2\pi r^2 \left(\alpha_{\text{GB},1} + \frac{2}{3}\alpha_3 \right) p + \frac{2}{3}\alpha_3 \right] M \right. \\ & \left. + \pi r^4 \left[(\alpha_{\text{GB},1} - \alpha_{\text{GB},2}) \left(\pi p r^2 - \frac{1}{4} \right) \rho - 2 \left(\pi\alpha_{\text{GB},1}r^2 p - \frac{1}{4}\alpha_{\text{GB},1} - \frac{1}{2}\alpha_3 \right) p \right] \right\} \left. + 6r^6\vartheta^{(0)'}(r-2M)^3\xi_0'' \right. \\ & + 1536r \left\{ \frac{1}{128}(2\pi r^3\rho - 2\pi p r^3 - r + M)(r-2M)r^4\vartheta^{(0)'} + \frac{3}{4}\alpha_3 M^3 - \frac{\alpha_3}{4} \left(7\pi\rho r^2 - \pi p r^2 + \frac{3}{2} \right) rM^2 \right. \\ & + \frac{\pi}{4}M r^4 \left\{ \pi(\alpha_{\text{GB},1} + 3\alpha_{\text{GB},2})r^2\rho^2 + \left[-13\pi \left(\alpha_{\text{GB},1} - \frac{11}{13}\alpha_{\text{GB},2} + \frac{12}{13}\alpha_3 \right) r^2 p + 4\alpha_3 \right] \rho \right. \\ & \left. + 10\pi \left(\alpha_{\text{GB},1} + \frac{2}{5}\alpha_3 \right) r^2 p^2 \right\} + \pi^2 r^7 \left\{ \pi(\alpha_{\text{GB},1} - \alpha_{\text{GB},2}) \left(r^2 p - \frac{1}{2}\alpha_{\text{GB},2} \right) \rho^2 \right. \\ & \left. - \left[\pi(\alpha_{\text{GB},1} + \alpha_{\text{GB},2})r^2 p - \frac{3}{2}\alpha_{\text{GB},1} + \frac{3}{2}\alpha_{\text{GB},2} - 2\alpha_3 \right] p \rho - 2\alpha_{\text{GB},1} \left(\pi p r^2 + \frac{3}{4} \right) p^2 \right\} \left. \right\} (r-2M)\xi_0' \\ & + 192 \left\{ \frac{1}{8}M^2\xi_0 - \frac{1}{2}r \left(\pi\rho r^2 - \pi p r^2 + \frac{1}{4} \right) \xi_0 M + r^2 \left[\pi^2 r^4 \rho^2 \xi_0 - \pi r^2 \rho \left(\pi r^2 p \xi_0 - \frac{m_0}{4} + \frac{\xi_0}{8} \right) \right. \right. \\ & \left. \left. - \frac{\pi}{8}r^2(\xi_0 + 2m_0)p + \frac{\xi_0}{16} - \frac{m_0}{16} \right] \right\} r^4(r-2M)\vartheta^{(0)'} + 5760\alpha_3 M^4 \xi_0 \\ & - 9984 \left(\pi r^2 \rho \xi_0 - \frac{\pi}{13}r^2 p \xi_0 + \frac{3}{26}m_0 + \frac{33}{52}\xi_0 \right) r\alpha_3 M^3 + 768 \left\{ \pi^2(\alpha_{\text{GB},1} - 3\alpha_{\text{GB},2})r^4 \rho \xi_0^2 \right. \\ & + 5\pi r^2 \rho \xi_0 \left[\pi \left(\alpha_{\text{GB},1} - \frac{7}{5}\alpha_{\text{GB},2} \right) r^2 p + \frac{18}{5}\alpha_3 \right] - 8\pi^2(\alpha_{\text{GB},1} + \alpha_3)r^4 p^2 \xi_0 - \pi\alpha_3 r^2 p \xi_0 + \frac{9}{4}\alpha_3(m_0 + \xi_0) \left. \right\} r^2 M^2 \\ & - 24576r^3 \left\{ -\frac{\pi^3}{4}\alpha_{\text{GB},2}r^6 \rho^3 \xi_0 + \pi^2 r^4 \rho^2 \left[\pi \left(\alpha_{\text{GB},1} - \alpha_{\text{GB},2} + \frac{1}{2}\alpha_3 \right) r^2 p \xi_0 + \left(\frac{1}{32}\alpha_{\text{GB},1} - \frac{1}{16}\alpha_{\text{GB},2} + \frac{3}{16}\alpha_3 \right) \xi_0 \right. \right. \\ & \left. \left. - \frac{1}{16}\alpha_{\text{GB},2}m_0 \right] - \left\{ \pi^2 \left(\alpha_{\text{GB},1} + \frac{1}{4}\alpha_{\text{GB},2} + \frac{1}{2}\alpha_3 \right) r^4 p^2 \xi_0 - \frac{\pi}{16}r^2 p \left[(\alpha_{\text{GB},1} - 2\alpha_{\text{GB},2}) \xi_0 \right. \right. \right. \\ & \left. \left. + 3m_0 \left(\alpha_{\text{GB},1} - \alpha_{\text{GB},2} + \frac{2}{3}\alpha_3 \right) \right] - \frac{3}{16}\alpha_3 \left(\xi_0 + \frac{m_0}{4} \right) \right\} \pi r^2 \rho - \frac{\pi^3}{2}\alpha_{\text{GB},1}r^6 p^3 \xi_0 \end{aligned}$$

$$\begin{aligned}
& - \frac{5}{32} \pi^2 r^4 p^2 \left[\left(\alpha_{\text{GB},1} + \frac{2}{5} \alpha_3 \right) \xi_0 + \frac{6}{5} \left(\alpha_{\text{GB},1} + \frac{2}{3} \alpha_3 \right) m_0 \right] - \frac{\pi}{64} \alpha_3 r^2 p m_0 + \frac{3}{128} \alpha_3 m_0 \Big\} M \\
& + 12288 \pi r^6 \left\{ \pi^2 r^4 \rho^3 \xi_0 \left[\pi (\alpha_{\text{GB},1} - \alpha_{\text{GB},2}) r^2 p + \frac{1}{8} \alpha_{\text{GB},1} - \frac{3}{8} \alpha_{\text{GB},2} \right] - \pi r^2 \rho^2 \left\{ \pi^2 (\alpha_{\text{GB},1} + \alpha_{\text{GB},2}) r^4 p^2 \xi_0 \right. \right. \\
& \left. \left. - \frac{3}{4} r^2 \pi p \left[\left(\alpha_{\text{GB},1} - \frac{4}{3} \alpha_{\text{GB},2} + \frac{4}{3} \alpha_3 \right) \xi_0 + \frac{1}{3} (\alpha_{\text{GB},1} - \alpha_{\text{GB},2}) m_0 \right] - \frac{1}{4} \alpha_3 \xi_0 - \frac{1}{32} (\alpha_{\text{GB},1} - 3 \alpha_{\text{GB},2}) m_0 \right\} \right. \\
& \left. + \left\{ -2r^6 \alpha_{\text{GB},1} \xi_0 \pi^3 p^3 - \frac{9}{8} \pi^2 \left[\left(\alpha_{\text{GB},1} + \frac{1}{9} \alpha_{\text{GB},2} \right) r^4 p^2 \xi_0 + \frac{2}{9} (\alpha_{\text{GB},1} + \alpha_{\text{GB},2}) m_0 \right] \right. \right. \\
& \left. \left. + \frac{5}{32} \pi \left(\alpha_{\text{GB},1} - \frac{7}{5} \alpha_{\text{GB},2} + \frac{8}{5} \alpha_3 \right) r^2 p m_0 + \frac{1}{16} \alpha_3 m_0 \right\} \rho - \frac{\pi}{4} \alpha_{\text{GB},1} r^2 p^2 (\pi r^2 p (\xi_0 + 2m_0) + m_0) \right\}, \quad (\text{A10})
\end{aligned}$$

where the primes represent derivatives with respect to r . ω_1 and m_0 are the $l = 1$ mode of the (t, ϕ) component and the $l = 0$ mode of the (r, r) component of the metric perturbation, while ξ_0 is the $l = 0$ mode of the perturbation

to the radial coordinate such that the perturbations to p and ρ vanish [108, 109]. Solving such an equation in the exterior region within the small coupling approximation, one finds the exterior solution for the scalar field:

$$\begin{aligned}
\vartheta_{0,\text{ext}}^{(2,1/2)}(r) = & \frac{1}{30M_*(r-2M_*)} \left\{ 15 \left[- \left(\mu^{(0,1/2)} M_*^2 - \alpha_3 \right) \chi^2 + 2\delta m \left(\mu^{(0,1/2)} M_*^2 - 4\alpha_3 \right) \right] \right. \\
& + 15 \left[\left(\mu^{(0,1/2)} M_*^2 - \alpha_3 \right) \chi^2 - 2 \left(\mu^{(0,1/2)} M_*^2 \xi_{0,*} - 4\alpha_3 \delta m \right) \right] \frac{M_*}{r} + 10 \left[\left(\mu^{(0,1/2)} M_*^2 - \alpha_3 \right) \chi^2 + 8\delta m \right] \frac{M_*^2}{r^2} \\
& + 10 \left[\left(\mu^{(0,1/2)} M_*^2 - \alpha_3 \right) \chi^2 - 16\delta m \right] \frac{M_*^3}{r^3} + 12 \left(40\xi_{0,*} - \chi^2 \right) \frac{M_*^4}{r^4} + 224\chi^2 \frac{M_*^5}{r^5} - 160\chi^2 \frac{M_*^6}{r^6} \\
& \left. - \frac{15}{2} \frac{r}{M_*} \left(1 - \frac{2M_*}{r} \right) \left[2\mu^{(2,1)} M_*^2 - 2\delta m \left(\mu^{(0,1/2)} M_*^2 - 4\alpha_3 \right) + \chi^2 \left(\mu^{(0,1/2)} M_*^2 - \alpha_3 \right) \right] \ln \left(1 - 2\frac{M_*}{r} \right) \right\}, \quad (\text{A11})
\end{aligned}$$

where $\mu^{(2,1/2)}$ is the only integration constant that corresponds to the dimensionless scalar charge at second order in spin and to leading order in ζ . δm is the fractional correction to the stellar mass at second order in rotation while $\xi_{0,*}$ corresponds to ξ_0/M at the surface. We have set ξ_0 in the exterior region to a constant, namely $\xi_{0,\text{ext}}(r) = \xi_0(R_*)$.

2. Numerical Scheme

Let us next explain the numerical algorithm that we use to calculate the scalar charge of slowly-rotating isotropic NSs with a variety of realistic equations of state in quadratic gravity. We assume the linear coupling function of the scalar field in Eq. (A6) and use the field equation and exterior solutions derived in Sec. A 1 b.

The equations of state we employ are the following tabulated ones: APR [120], SLy [121], LS220 [122], Shen [123, 124] and WFF1 [125]. These equations of state are found by solving certain many-body quantum field theory equations for the internal pressure and density at supra-nuclear densities. Due to the difficulty of solving

these equations and uncertainties about the strength of certain interactions, different approximations are made that lead to different equations of state. We also continue to consider an $n = 0$ polytropic equation of state and a Tolman VII model to allow for comparisons with the analytical study section.

A numerical solution to the scalar field evolution equation requires boundary conditions. We choose to specify these at the stellar center through a local analysis of the

differential equation, which leads to

$$\begin{aligned} \vartheta^{(0,1/2)} &= \vartheta_c^{(0,1/2)} - \frac{32\pi^2}{9R_*^2} \left[(3\alpha_{\text{GB},2} - 4\alpha_3) \right. \\ &\quad \left. - 6(3\alpha_1 - \alpha_3) \frac{p_c}{\rho_c} + 9\alpha_{\text{GB},1} \left(\frac{p_c}{\rho_c} \right)^2 \right] x^2 \\ &\quad + \mathcal{O}(x^3), \end{aligned} \quad (\text{A12})$$

$$\begin{aligned} \vartheta_0^{(2,1/2)} &= \vartheta_{0,c}^{(2,1/2)} - \frac{16\pi}{9R_*^2} \frac{\omega_{1,c}^2 e^{-\nu_c}}{\rho_c + 3p_c} \left[(3\alpha_{\text{GB},2} - 4\alpha_3) \right. \\ &\quad \left. - 6(3\alpha_1 - \alpha_3) \frac{p_c}{\rho_c} + 9\alpha_{\text{GB},1} \left(\frac{p_c}{\rho_c} \right)^2 \right] x^2 \\ &\quad + \mathcal{O}(x^3), \end{aligned} \quad (\text{A13})$$

where $\nu = \nu(r)$ and $\omega_1 = \omega_1(r)$ are metric functions at zeroth- and first-order in rotation. We have defined the expansion parameter $x \equiv R_* r \rho_c \ll 1$ and where the subscript c stands for the value of the function at the stellar center. We initiate our integrations at a core radius $r = r_c > 0$, whose value we choose ensuring the local analysis presented above is valid, namely $R_* \rho_c r_c \ll 1$. For example, setting $R_* = 12$ km and $\rho_c = 10^{15}$ g/cm³, which is the typical NS central density, the constraint $x(r = r_c) \ll 1$ implies $r_c \ll 10^7$ cm; we choose here $r_c = 10$ cm which satisfies this bound.

The interior solution to the scalar field evolution equation can be found numerically as follows. First, we choose an arbitrary trial value for the boundary value constants ($\vartheta_c^{(0,1/2)}$, $\vartheta_{0,c}^{(2,1/2)}$), with which we find homogeneous ($\vartheta_{\text{H}}^{(0,1/2)}$, $\vartheta_{0,\text{H}}^{(2,1/2)}$) and particular ($\vartheta_{\text{P}}^{(0,1/2)}$, $\vartheta_{0,\text{P}}^{(2,1/2)}$) solutions through a fourth-order Runge-Kutta integrator. The solution that satisfies the proper boundary conditions at the stellar surface must then be a linear combination of these two solutions, namely

$$\vartheta^{(0,1/2)} = C_{\vartheta}^{(0)} \vartheta_{\text{H}}^{(0,1/2)} + \vartheta_{\text{P}}^{(0,1/2)}, \quad (\text{A14})$$

$$\vartheta_0^{(2,1/2)} = C_{\vartheta}^{(2)} \vartheta_{0,\text{H}}^{(2,1/2)} + \vartheta_{0,\text{P}}^{(2,1/2)}, \quad (\text{A15})$$

where $C_{\vartheta}^{(A)}$ ($A = 0, 2$) is an integration constant to be determined by matching at the stellar surface.

With the interior and exterior solutions at hand with the latter given by Eqs. (A9) and (A11), we match them at the stellar surface at each order in $M_* \Omega$. At zeroth-order in rotation, the matching condition is simply

$$\vartheta^{(0,1/2)}(R_*) = \vartheta_{\text{ext}}^{(0,1/2)}(R_*), \quad \vartheta^{(0,1/2)'}(R_*) = \vartheta_{\text{ext}}^{(0,1/2)'}(R_*), \quad (\text{A16})$$

where the primes denote differentiation with respect to r . In this paper, we choose the radial deformation function ξ_0 in the exterior region to be constant as $\xi_{0,\text{ext}}(r) = \xi_0(R_*)$. In such a case, the matching condition at second-order in rotation is

$$\vartheta_0^{(2,1/2)}(R_*) = \vartheta_{0,\text{ext}}^{(2,1/2)}(R_*), \quad (\text{A17})$$

$$\vartheta_0^{(2,1/2)'}(R_*) = \vartheta_{0,\text{ext}}^{(2,1/2)'}(R_*) + \vartheta_{0,\text{ext}}^{(0,1/2)'}(R_*) \xi_0^{(2)'}(R_*). \quad (\text{A18})$$

The second term in Eq. (A18) is required to ensure smoothness of the scalar field at the stellar surface and it is induced by the non-smoothness of $\xi_0^{(2)}$ at the stellar surface. These four conditions determine $C_{\vartheta}^{(A)}$ and $\mu^{(A)}$ at each order in rotation.

3. Strongly Anisotropic Neutron Stars

Let us finally explain how one can show that the scalar charge vanishes in D²GB gravity for strongly anisotropic NSs without using the post-Minkowskian expansion. Such a star can be modeled through a stress-energy tensor of the form [126, 127]

$$T_{\mu\nu} = \rho u_{\mu} u_{\nu} + p_r k_{\mu} k_{\nu} + q_t \Pi_{\mu\nu}, \quad (\text{A19})$$

where k^{μ} is the unit radial four-vector orthogonal to the timelike four-velocity vector u^{μ} and

$$\Pi_{\mu\nu} = g_{\mu\nu} + u_{\mu} u_{\nu} - k_{\mu} k_{\nu} \quad (\text{A20})$$

is a projection operator onto a two-surface orthogonal to u^{μ} and k^{μ} . The quantity $p_r = p_r(r, \theta)$ is the radial pressure function, while $q_t = q_t(r, \theta)$ is the tangential pressure function, so that $\sigma = \sigma(r, \theta) \equiv p_r(r, \theta) - q_t(r, \theta)$ is an anisotropy parameter function. Clearly, the limit $\sigma \rightarrow 0$ corresponds to isotropic matter [126, 127].

Are NSs expected to be anisotropic? Clearly, some degree of anisotropy should be present, for example due to magnetic fields or superfluidity. But such anisotropy is expected to be small, which translates to the functional constraint $\sigma/p_r \ll 1$. Precisely how much anisotropy is present in NSs and how this anisotropy manifests itself mathematically is not clear. The framework described above should thus be considered a toy model. We study it here because it turns out to allow for analytic, closed-form solutions to the equations of structure in spherical symmetry for the metric functions without requiring a subsequent post-Minkowskian expansion.

Let us then work to zeroth order in rotation—in spherical symmetry [126, 127]. The scalar field evolution equation in Eq. (60) acquires an anisotropic term $S_{\sigma}^{(0)}$. With the linear scalar coupling in Eq. (A6), $S_{\sigma}^{(0)}$ is given by

$$\begin{aligned} S_{\sigma}^{(0)} &= \frac{128\pi [2\pi\alpha_{\text{GB},1} r^3 p - \alpha_3 M - 2\pi(\alpha_1 - \alpha_3) r^3 \rho]}{r^2(r - 2M)} \sigma \\ &\quad - \frac{64\pi^2 (\alpha_{\text{GB},1} + \alpha_{\text{GB},2}) r}{(r - 2M)} \sigma^2. \end{aligned} \quad (\text{A21})$$

Observe that $S_{\sigma}^{(0)}$ does not vanish in the Gauss-Bonnet limit.

Before we can proceed, we must now choose a particular model for the anisotropy parameter function σ . We adopt here the model proposed in [107], namely

$$\sigma = \frac{\lambda_{\text{BL}}}{3} (\rho + 3p)(\rho + p) \left(1 - \frac{2M}{r} \right)^{-1} r^2, \quad (\text{A22})$$

where λ_{BL} is a dimensionless parameter that quantifies the amount of anisotropy. The isotropic pressure case corresponds to setting $\lambda_{\text{BL}} = 0$, while the lower limit on λ_{BL} is given by $\lambda_{\text{BL}} = -2\pi$, beyond which the maximum compactness becomes negative and unphysical [107]. Such a model was specifically constructed so that the equations of structure in spherical symmetry can be solved in closed-form for an $n = 0$ polytropic equation of state, without requiring a post-Minkowskian expansion [107].

Let us now solve the scalar field evolution equation for anisotropic stars. We further specialize the scalar field equation to the Gauss-Bonnet limit by setting $(\alpha_1, \alpha_2, \alpha_3) = \alpha_{\text{GB}}(1, -4, 1)$, where α_{GB} is now the only free parameter; without this specialization, the scalar field equation is too difficult to solve in closed-form without a post-Minkowskian expansion. We also take the strongly anisotropic limit of $\lambda_{\text{BL}} \rightarrow -2\pi$, in which the radial pressure vanishes throughout the constant density ($n = 0$) star. The scalar field equation then simplifies to

$$\frac{d^2\vartheta^{(0,1/2)}}{dr^2} = -\frac{5Cr^2 - 2R_*^2}{(2Cr^2 - R_*^2)r} \frac{d\vartheta^{(0,1/2)}}{dr} - \frac{48\ell^2\alpha_{\text{GB}}C^2(Cr^2 - R_*^2)}{(2Cr^2 - R_*^2)^2R_*^2}, \quad (\text{A23})$$

where we used the small coupling approximation. In the interior region, the solution to Eq. (A23) is

$$\vartheta^{(0,1/2)} = -\frac{4\alpha_{\text{GB}}C}{R_*^2} \ln(R_*^2 - 2Cr^2) + \vartheta_c^{(0,1/2)}, \quad (\text{A24})$$

where $\vartheta_c^{(0,1/2)}$ is the only integration constant because we have imposed regularity at the center. Matching this interior solution with the exterior one in Eq. (A9) and their first-derivatives at the stellar surface then automatically forces $\mu^{(0,1/2)} = 0$.

Appendix B: Corrections to Neutron Star Binary Evolution in Shift-Symmetric Topological Quadratic Gravity

In this appendix, we derive the quadratic gravity correction to a NS binary within the shift-symmetric, topological class of quadratic gravity theories. As an example, we consider D²GB gravity. We look at the conservative and dissipative corrections due to the scalar field and metric deformation in turn.

1. Corrections due to the Scalar Field

Let us first consider corrections to the dynamics of binary systems without BHs caused *directly* by the scalar field. To do this, we first need to determine the leading-order asymptotic behavior of the scalar field at spatial infinity. When the scalar charge vanishes, $\vartheta^{(0,1/2)}$ and

$\vartheta_0^{(2,1/2)}$ are completely sourced by the particular solutions to the scalar field evolution equation and their asymptotic behavior at spatial infinity becomes

$$\vartheta^{(0,1/2)}(r) = -4\frac{\alpha_{\text{GB}}}{M_*^2} \left(\frac{M_*}{r}\right)^4 + \mathcal{O}\left(\frac{M_*^5}{r^5}\right), \quad (\text{B1})$$

$$\vartheta_0^{(2,1/2)}(r) = -8\delta m \frac{\alpha_{\text{GB}}}{M_*^2} \left(\frac{M_*}{r}\right)^4 + \mathcal{O}\left(\frac{M_*^5}{r^5}\right). \quad (\text{B2})$$

On the other hand, the asymptotic behavior of $\vartheta_2^{(2,1/2)}$ at spatial infinity is

$$\vartheta_2^{(2,1/2)}(r) = \mu_2^{(2,1/2)} \left(\frac{M_*}{r}\right)^3 + \mathcal{O}\left(\frac{M_*^4}{r^4}\right), \quad (\text{B3})$$

where $\mu_2^{(2,1/2)}$ corresponds to the dimensionless scalar quadrupole charge, as predicted in [25]. Clearly, the scalar quadrupole charge is dominant at spatial infinity if it is non-vanishing.

Let us now consider scalar field corrections to the conservative dynamics of binary systems, i.e. to the Hamiltonian or the binary's binding energy. The correction to the latter due to a scalar quadrupole-quadrupole interaction is given by [25]:

$$E_b^\vartheta \propto \left(\frac{m}{r_{12}}\right)^5, \quad (\text{B4})$$

where m and r_{12} are the total mass and binary separation respectively. Comparing this to the Newtonian potential ($E_b = m/r_{12}$), it is clear that this deformation enters at relative 4PN order.

Let us now consider scalar field corrections to the dissipative dynamics of binary systems, i.e. to the energy fluxes carried away by a dynamical scalar field with quadrupole scalar charge. Following [24], one can show that the dominant contribution comes from e.g. the scalar field coupled to the metric perturbation in $\square\vartheta$ as

$$\dot{E}^\vartheta \propto (v_{12})^{18}. \quad (\text{B5})$$

Comparing this to the leading-order energy flux in general relativity ($\dot{E}_{\text{GR}} \propto (v_{12})^{10}$), it is clear that this deformation enters at 4PN order.

2. Corrections due to the Metric Deformation

Let us now consider corrections to the dynamics of NS/NS binary systems caused *indirectly* by the scalar field, due to how this induces a deformation in the metric.

Consider first the conservative sector of the dynamics of binaries. The binding energy is constructed directly from the metric tensor in the *near-zone*, i.e. at distances smaller than the GW wavelength of the binary. Since the quadrupole moment of each NS is modified due to a non-vanishing scalar quadrupole hair, the near-zone

metric will acquire corrections proportional to $1/r_{12}^3$, which will then propagate into the binding energy. This then implies that the metric deformation causes a 2PN correction to the energy [28].

Consider now the dissipative sector of the dynamics. The dominant effect of the modification to the energy and angular momentum fluxes carried away by the dynamical part of the metric perturbation comes from e.g. the effective source term that gives the correct quadrupole moment deformation. Following the analysis of [24], one

can show that such a dynamical metric perturbation will be proportional to

$$|\delta h_{ij}| \propto \frac{m}{r} (v_{12})^8. \quad (\text{B6})$$

Comparing this to the magnitude of GWs in general relativity ($|h_{ij}| \propto (m/r)(v_{12})^2$), we conclude that these deformations induce a modification in the dissipative dynamics of 3PN relative order.

-
- [1] C. M. Will, *Living Reviews in Relativity* **17** (2014), 10.12942/lrr-2014-4, arXiv:1403.7377.
- [2] N. Yunes and X. Siemens, *Living Rev.Rel.* **16**, 9 (2013), arXiv:1304.3473 [gr-qc].
- [3] M. Milgrom, *Astrophys.J.* **270**, 365 (1983).
- [4] R. H. Sanders and S. S. McGaugh, *Ann.Rev.Astron.Astrophys.* **40**, 263 (2002), arXiv:astro-ph/0204521 [astro-ph].
- [5] J. D. Bekenstein, *Phys.Rev.* **D70**, 083509 (2004), arXiv:astro-ph/0403694 [astro-ph].
- [6] B. Famaey and S. McGaugh, *Living Rev.Rel.* **15**, 10 (2012), arXiv:1112.3960 [astro-ph.CO].
- [7] L. Amendola and S. Tsujikawa, *Dark Energy: Theory and Observations* (Cambridge University Press, 2010).
- [8] A. De Felice and S. Tsujikawa, *Living Rev.Rel.* **13**, 3 (2010), arXiv:1002.4928 [gr-qc].
- [9] C. de Rham, *Living Rev.Rel.* **17**, 7 (2014), arXiv:1401.4173 [hep-th].
- [10] J. Polchinski, *String theory. Vol. 1: An introduction to the bosonic string* (Cambridge University Press, Cambridge, UK, 1998).
- [11] J. Polchinski, *String theory. Vol. 2: Superstring theory and beyond* (Cambridge University Press, Cambridge, UK, 1998).
- [12] Y. Fujii and K. Maeda, *The scalar-tensor theory of gravitation* (Cambridge University Press, 2007).
- [13] R. Jackiw and S. Y. Pi, *Phys. Rev.* **D68**, 104012 (2003), arXiv:gr-qc/0308071.
- [14] S. Alexander and N. Yunes, *Phys. Rept.* **480**, 1 (2009), arXiv:0907.2562 [hep-th].
- [15] S. H. S. Alexander and S. J. Gates, Jr., *JCAP* **0606**, 018 (2006), arXiv:hep-th/0409014.
- [16] V. Taveras and N. Yunes, *Phys. Rev.* **D78**, 064070 (2008), arXiv:0807.2652 [gr-qc].
- [17] S. Mercuri and V. Taveras, *Phys. Rev.* **D80**, 104007 (2009), arXiv:0903.4407 [gr-qc].
- [18] S. Weinberg, *Phys. Rev.* **D77**, 123541 (2008), arXiv:0804.4291 [hep-th].
- [19] T. Damour and G. Esposito-Farese, *Phys. Rev.* **D54**, 1474 (1996), arXiv:gr-qc/9602056 [gr-qc].
- [20] I. H. Stairs, *Living Rev.Rel.* **6**, 5 (2003).
- [21] M. Kramer, I. H. Stairs, R. Manchester, M. McLaughlin, A. Lyne, *et al.*, *Science* **314**, 97 (2006), arXiv:astro-ph/0609417 [astro-ph].
- [22] P. C. Freire *et al.*, *Mon.Not.Roy.Astron.Soc.* **423**, 3328 (2012), arXiv:1205.1450 [astro-ph.GA].
- [23] N. Wex, in *Frontiers in Relativistic Celestial Mechanics*, Vol. 1, edited by S. Kopeikin (De Gruyter, 2014) arXiv:1402.5594 [gr-qc].
- [24] K. Yagi, L. C. Stein, N. Yunes, and T. Tanaka, *Phys.Rev.* **D85**, 064022 (2012), arXiv:1110.5950 [gr-qc].
- [25] L. C. Stein and K. Yagi, *Phys.Rev.* **D89**, 044026 (2014), arXiv:1310.6743 [gr-qc].
- [26] R. Jackiw and S. Y. Pi, *Phys. Rev.* **D68**, 104012 (2003), gr-qc/0308071.
- [27] K. Yagi, N. Yunes, and T. Tanaka, *Phys.Rev.Lett.* **109**, 251105 (2012), arXiv:1208.5102 [gr-qc].
- [28] K. Yagi, L. C. Stein, N. Yunes, and T. Tanaka, *Phys.Rev.* **D87**, 084058 (2013), arXiv:1302.1918 [gr-qc].
- [29] E. Barausse and K. Yagi, *Phys. Rev. Lett.* **115**, 211105 (2015), arXiv:1509.04539 [gr-qc].
- [30] N. Yunes and L. C. Stein, *Phys. Rev. D* **83**, 104002 (2011), arXiv:1101.2921 [gr-qc].
- [31] B. A. Campbell, N. Kaloper, and K. A. Olive, *Physics Letters B* **285**, 199 (1992).
- [32] S. Mignemi and N. Stewart, *Phys.Rev.* **D47**, 5259 (1993), arXiv:hep-th/9212146 [hep-th].
- [33] T. P. Sotiriou and S.-Y. Zhou, *Phys.Rev.* **D90**, 124063 (2014), arXiv:1408.1698 [gr-qc].
- [34] S. W. Hawking, *Comm. Math. Phys.* **25**, 167 (1972).
- [35] T. P. Sotiriou and V. Faraoni, *Phys.Rev.Lett.* **108**, 081103 (2012), arXiv:1109.6324 [gr-qc].
- [36] A. A. H. Graham and R. Jha, *Phys.Rev.* **D90**, 041501 (2014), arXiv:1407.6573 [gr-qc].
- [37] P. G. Bergmann, *Int. J. Theor. Phys.* **1**, 25 (1968).
- [38] R. V. Wagoner, *Phys. Rev.* **D1**, 3209 (1970).
- [39] J. Healy, T. Bode, R. Haas, E. Pazos, P. Laguna, *et al.*, *Class.Quant.Grav.* **29**, 232002 (2012), arXiv:1112.3928 [gr-qc].
- [40] T. Jacobson, *Phys.Rev.Lett.* **83**, 2699 (1999), arXiv:astro-ph/9905303 [astro-ph].
- [41] M. Horbatsch and C. Burgess, *JCAP* **1205**, 010 (2012), arXiv:1111.4009 [gr-qc].
- [42] C. M. Will and H. W. Zaglauer, *Astrophys.J.* **346**, 366 (1989).
- [43] C. M. Will, *Phys. Rev.* **D50**, 6058 (1994), arXiv:gr-qc/9406022 [gr-qc].
- [44] T. Damour and G. Esposito-Farese, *Phys. Rev.* **D58**, 042001 (1998), arXiv:gr-qc/9803031 [gr-qc].
- [45] J. Alsing, E. Berti, C. M. Will, and H. Zaglauer, *Phys.Rev.* **D85**, 064041 (2012), arXiv:1112.4903 [gr-qc].
- [46] L. Sampson, N. Yunes, N. Cornish, M. Ponce, E. Barausse, *et al.*, *Phys.Rev.* **D90**, 124091 (2014), arXiv:1407.7038 [gr-qc].
- [47] L. Hui and A. Nicolis, *Phys. Rev. Lett.* **110**, 241104 (2013), arXiv:1202.1296 [hep-th].
- [48] A. Maselli, H. O. Silva, M. Minamitsuji, and E. Berti, (2015), arXiv:1508.03044 [gr-qc].

- [49] K. Yagi, *Phys. Rev.* **D86**, 081504 (2012), arXiv:1204.4524 [gr-qc].
- [50] P. Kanti, N. Mavromatos, J. Rizos, K. Tamvakis, and E. Winstanley, *Phys.Rev.* **D54**, 5049 (1996), arXiv:hep-th/9511071 [hep-th].
- [51] P. Pani and V. Cardoso, *Phys.Rev.* **D79**, 084031 (2009), arXiv:0902.1569 [gr-qc].
- [52] “LIGO,” <http://www.ligo.caltech.edu/>.
- [53] A. Abramovici *et al.*, *Science* **256**, 325 (1992).
- [54] B. Abbott *et al.* (LIGO Scientific), *Rept.Prog.Phys.* **72**, 076901 (2009), arXiv:0711.3041 [gr-qc].
- [55] “VIRGO,” <http://www.virgo.infn.it/>.
- [56] A. Giazotto, *Nucl.Instrum.Meth.* **A289**, 518 (1990).
- [57] F. Acernese *et al.* (Virgo Collaboration), *Class.Quant.Grav.* **32**, 024001 (2015), arXiv:1408.3978 [gr-qc].
- [58] C. L. Carilli and S. Rawlings, *New Astron.Rev.* **48**, 979 (2004), arXiv:astro-ph/0409274 [astro-ph].
- [59] G. Esposito-Farese, in *38th Rencontres de Moriond on Gravitational Waves and Experimental Gravity Les Arcs, Savoie, France, March 22-29, 2003* (2003) arXiv:gr-qc/0306018 [gr-qc].
- [60] L. Amendola, C. Charmousis, and S. C. Davis, *JCAP* **0710**, 004 (2007), arXiv:0704.0175 [astro-ph].
- [61] T. P. Sotiriou and E. Barausse, *Phys.Rev.* **D75**, 084007 (2007), arXiv:gr-qc/0612065 [gr-qc].
- [62] S. Alexander and N. Yunes, *Phys. Rev. Lett.* **99**, 241101 (2007), arXiv:hep-th/0703265.
- [63] S. Alexander and N. Yunes, *Phys.Rev.* **D75**, 124022 (2007), arXiv:0704.0299 [hep-th].
- [64] T. L. Smith, A. L. Erickcek, R. R. Caldwell, and M. Kamionkowski, *Phys. Rev.* **D77**, 024015 (2008), arXiv:0708.0001 [astro-ph].
- [65] K. Yagi, *Phys.Rev.* **D86**, 081504 (2012), arXiv:1204.4524 [gr-qc].
- [66] K. Yagi and N. Yunes, *Science* **341**, 365 (2013), arXiv:1302.4499 [gr-qc].
- [67] K. Yagi and N. Yunes, *Phys. Rev. D* **88**, 023009 (2013), arXiv:1303.1528 [gr-qc].
- [68] C. F. Sopuerta and N. Yunes, *Phys.Rev.* **D80**, 064006 (2009), arXiv:0904.4501 [gr-qc].
- [69] P. Pani, V. Cardoso, and L. Gualtieri, *Phys. Rev.* **D83**, 104048 (2011), arXiv:1104.1183 [gr-qc].
- [70] P. Canizares, J. R. Gair, and C. F. Sopuerta, *Phys.Rev.* **D86**, 044010 (2012), arXiv:1205.1253 [gr-qc].
- [71] T. Harko, Z. Kovacs, and F. S. N. Lobo, *Class. Quant. Grav.* **27**, 105010 (2010), arXiv:0909.1267 [gr-qc].
- [72] L. Amarilla, E. F. Eiroa, and G. Giribet, *Phys. Rev.* **D81**, 124045 (2010), arXiv:1005.0607 [gr-qc].
- [73] S. Chen and J. Jing, *Class. Quant Grav.* **27**, 225006 (2010), arXiv:1005.1325 [gr-qc].
- [74] P. Jordan, *Z.Phys.* **157**, 112 (1959).
- [75] C. Brans and R. H. Dicke, *Phys. Rev.* **124**, 925 (1961).
- [76] E. Berti, E. Barausse, V. Cardoso, L. Gualtieri, P. Pani, *et al.*, (2015), arXiv:1501.07274 [gr-qc].
- [77] J. K. Bloomfield and E. E. Flanagan, *JCAP* **1210**, 039 (2012), arXiv:1112.0303 [gr-qc].
- [78] D. J. Gross and J. H. Sloan, *Nucl.Phys.* **B291**, 41 (1987).
- [79] R. Metsaev and A. A. Tseytlin, *Nucl.Phys.* **B293**, 385 (1987).
- [80] S. Mignemi, *Phys.Rev.* **D51**, 934 (1995), arXiv:hep-th/9303102 [hep-th].
- [81] B. Kleihaus, J. Kunz, and E. Radu, *Phys.Rev.Lett.* **106**, 151104 (2011), arXiv:1101.2868 [gr-qc].
- [82] S. Alexander and N. Yunes, *Phys. Rev.* **D77**, 124040 (2008), arXiv:0804.1797 [gr-qc].
- [83] K.-i. Maeda, N. Ohta, and Y. Sasagawa, *Phys.Rev.* **D80**, 104032 (2009), arXiv:0908.4151 [hep-th].
- [84] C. P. Burgess, *Ann. Rev. Nucl. Part. Sci.* **57**, 329 (2007), arXiv:hep-th/0701053 [hep-th].
- [85] S. Dyda, E. E. Flanagan, and M. Kamionkowski, *Phys. Rev.* **D86**, 124031 (2012), arXiv:1208.4871 [gr-qc].
- [86] T. Delsate, D. Hilditch, and H. Witek, *Phys.Rev.* **D91**, 024027 (2015), arXiv:1407.6727 [gr-qc].
- [87] S. Deser, R. Jackiw, and S. Templeton, *Annals Phys.* **140**, 372 (1982).
- [88] S. Deser, R. Jackiw, and S. Templeton, *Phys.Rev.Lett.* **48**, 975 (1982).
- [89] N. Yunes and F. Pretorius, *Phys. Rev.* **D79**, 084043 (2009), arXiv:0902.4669 [gr-qc].
- [90] R. P. Woodard, *Lect.Notes Phys.* **720**, 403 (2007), arXiv:astro-ph/0601672 [astro-ph].
- [91] C. Burgess, *Living Rev.Rel.* **7**, 5 (2004), arXiv:gr-qc/0311082 [gr-qc].
- [92] M. Campanelli, C. O. Lousto, and J. Audretsch, *Phys. Rev.* **D49**, 5188 (1994), arXiv:gr-qc/9401013 [gr-qc].
- [93] A. Cooney, S. DeDeo, and D. Psaltis, *Phys. Rev.* **D82**, 064033 (2010), arXiv:0910.5480 [astro-ph.HE].
- [94] Y. Ali-Haimoud and Y. Chen, *Phys.Rev.* **D84**, 124033 (2011), arXiv:1110.5329 [astro-ph.HE].
- [95] K. Yagi, N. Yunes, and T. Tanaka, *Phys.Rev.* **D86**, 044037 (2012), arXiv:1206.6130 [gr-qc].
- [96] R. Wald, *General Relativity* (The University of Chicago Press, Chicago, 1984).
- [97] J. Stewart, *Advanced General Relativity*, Cambridge Monographs on Mathematical Physics (Cambridge University Press, 1993).
- [98] A. Avez, *C. R. Acad. Sci. Paris* **255**, 2049 (1962).
- [99] S.-S. Chern, *An. Acad. Brasil. Ci.* **35**, 17 (1963).
- [100] L. Alty, *J.Math.Phys.* **36**, 3094 (1995).
- [101] P. Gilkey and J. Park, *J.Gem.Phys.* **88**, 88 (2014).
- [102] B. Kleihaus, J. Kunz, and S. Mojica, *Phys.Rev.* **D90**, 061501 (2014), arXiv:1407.6884 [gr-qc].
- [103] G. M. Volkoff, *Physical Review* **55**, 413 (1939).
- [104] R. C. Tolman, *Phys.Rev.* **55**, 364 (1939).
- [105] L. Tsui and P. Leung, *Astrophys.J.* **631**, 495 (2005), arXiv:gr-qc/0505113 [gr-qc].
- [106] P. Pani, E. Berti, V. Cardoso, and J. Read, *Phys.Rev.* **D84**, 104035 (2011), arXiv:1109.0928 [gr-qc].
- [107] R. L. Bowers and E. P. T. Liang, *Astrophys. J.* **188**, 657 (1974).
- [108] J. B. Hartle, *Astrophys.J.* **150**, 1005 (1967).
- [109] J. B. Hartle and K. S. Thorne, *Astrophys. J.* **153**, 807 (1968).
- [110] N. Yunes and F. Pretorius, *Phys.Rev.* **D80**, 122003 (2009), arXiv:0909.3328 [gr-qc].
- [111] N. Cornish, L. Sampson, N. Yunes, and F. Pretorius, *Phys.Rev.* **D84**, 062003 (2011), arXiv:1105.2088 [gr-qc].
- [112] J. M. Lattimer and B. F. Schutz, *Astrophys.J.* **629**, 979 (2005), arXiv:astro-ph/0411470 [astro-ph].
- [113] K. Liu, N. Wex, M. Kramer, J. Cordes, and T. Lazio, *Astrophys.J.* **747**, 1 (2012), arXiv:1112.2151 [astro-ph.HE].
- [114] K. Liu, R. Eatough, N. Wex, and M. Kramer, *Mon.Not.Roy.Astron.Soc.* **445**, 3115 (2014), arXiv:1409.3882 [astro-ph.GA].
- [115] R. Nan, D. Li, C. Jin, Q. Wang, L. Zhu, *et al.*,

- Int.J.Mod.Phys. **D20**, 989 (2011), arXiv:1105.3794 [astro-ph.IM].
- [116] J. Antoniadis, P. C. Freire, N. Wex, T. M. Tauris, R. S. Lynch, *et al.*, *Science* **340**, 6131 (2013), arXiv:1304.6875 [astro-ph.HE].
- [117] T. Damour and G. Esposito-Farese, *Class.Quant.Grav.* **9**, 2093 (1992).
- [118] K. Yagi, D. Blas, E. Barausse, and N. Yunes, *Phys.Rev.* **D89**, 084067 (2014), arXiv:1311.7144 [gr-qc].
- [119] “GRTensorII,” This is a package which runs within Maple but distinct from packages distributed with Maple. It is distributed freely on the World-Wide-Web from the address <http://grtensor.org/>.
- [120] A. Akmal, V. Pandharipande, and D. Ravenhall, *Phys.Rev.* **C58**, 1804 (1998), arXiv:nucl-th/9804027 [nucl-th].
- [121] F. Douchin and P. Haensel, *Astron. Astrophys.* **380**, 151 (2001).
- [122] J. M. Lattimer and F. Douglas Swesty, *Nuclear Physics A* **535**, 331 (1991).
- [123] H. Shen, H. Toki, K. Oyamatsu, and K. Sumiyoshi, *Nuclear Physics A* **637**, 435 (1998).
- [124] H. Shen, H. Toki, K. Oyamatsu, and K. Sumiyoshi, *Progress of Theoretical Physics* **100**, 1013 (1998).
- [125] R. B. Wiringa, V. Fiks, and A. Fabrocini, *Phys.Rev.* **C38**, 1010 (1988).
- [126] D. D. Doneva and S. S. Yazadjiev, *Phys.Rev.* **D85**, 124023 (2012), arXiv:1203.3963 [gr-qc].
- [127] H. O. Silva, C. F. B. Macedo, E. Berti, and L. C. B. Crispino, *Class. Quant. Grav.* **32**, 145008 (2015), arXiv:1411.6286 [gr-qc].